

NIST Technical Note 2183

Reduced-Scale Compartment Gaseous Fuels Backdraft Experiments

Christopher U. Brown
Ryan Falkenstein-Smith
Thomas G. Cleary

This publication is available free of charge from:
<https://doi.org/10.6028/NIST.TN.2183>

NIST
**National Institute of
Standards and Technology**
U.S. Department of Commerce

NIST Technical Note 2183

Reduced-Scale Compartment Gaseous Fuels Backdraft Experiments

Christopher U. Brown
Ryan Falkenstein-Smith
Thomas G. Cleary
*Fire Research Division
Engineering Laboratory*

This publication is available free of charge from:
<https://doi.org/10.6028/NIST.TN.2183>

November 2021



U.S. Department of Commerce
Gina M. Raimondo, Secretary

National Institute of Standards and Technology
*James K. Olthoff, Performing the Non-Exclusive Functions and Duties of the Under Secretary of Commerce for
Standards and Technology & Director, National Institute of Standards and Technology*

Certain commercial entities, equipment, or materials may be identified in this document in order to describe an experimental procedure or concept adequately. Such identification is not intended to imply recommendation or endorsement by the National Institute of Standards and Technology, nor is it intended to imply that the entities, materials, or equipment are necessarily the best available for the purpose.

The opinions, recommendations, findings, and conclusions in this publication do not necessarily reflect the views or policies of NIST or the United States Government.

National Institute of Standards and Technology Technical Note 2183
Natl. Inst. Stand. Technol. Tech. Note 2183, 72 pages (November 2021)
CODEN: NTNOEF

This publication is available free of charge from:
<https://doi.org/10.6028/NIST.TN.2183>

Abstract

This report documents the design and construction of a reduced-scale compartment and summary data for a set of gaseous fuel experiments to study the backdraft phenomenon. In these experiments, a fire was enclosed in a compartment with modified configurations (e.g., fire size, fuel-off time, spark ignition location, spark delay time, and front opening) to identify precursors to a backdraft event. A moderate fire size of 25 kW was studied using methane, propane, and propene as individual fuels. A 16.7 kW propane fire and 37.5 kW methane fire were also studied. Temperature readings in the upper and lower layers of the compartment, pressure, external heat flux measurements, and heat flux measurements at the compartment floor were recorded during each experiment. For experiments where a backdraft occurred, flame size measurements and ignition times relative to the doorway opening were obtained from video recordings during the experiments. Experiments were repeated at least once for each set of selected experimental conditions. Fuel flow conditions for each fuel and fire size produced events ranging from no ignition to backdrafts for the range of compartment configurations studied. In general, the transition from no ignition to increasingly larger backdrafts was observed for each fuel as its flow time was increased.

Key words

Backdraft; Gaseous fuels; Reduced-Scale Compartment.

Table of Contents

1. Introduction	1
2. Methods	4
2.1. The Reduced-Scale Compartment.....	4
2.2. Pressure Relief Panel.....	5
2.3. Front Door and Window Configuration	7
2.4. Gas Fuel System.....	9
2.5. Spark Ignitors	12
2.6. Thermocouples	14
2.7. Heat Flux Gauge.....	16
2.8. Pressure Transducer	17
2.9. Gas Sampling	18
2.10. Data Acquisition System.....	18
2.11. General Experiment Procedure	19
2.12. Video Measurements of Backdraft Geometry.....	20
3. Results and Discussion	23
3.1. Backdraft Events and Non-events.....	23
3.2. Measurements from Experiments.....	34
4. Conclusion	52
References.....	53
Appendix A: Design Document Details.....	55

List of Tables

Table 1. Timeline of critical experiment occurrences.....	20
Table 2. Measurements for the 25.0 kW methane experiments with a door configuration and a low spark position.	35
Table 3. Measurements for the 25.0 kW methane experiments with a door configuration and a middle spark position.	36
Table 4. Measurements made for the 25.0 kW methane experiments with a window configuration and a low spark position.....	37
Table 5. Measurements for the 25.0 kW methane experiments with a window configuration and a middle spark position.	38
Table 6. Measurements for the 37.5 kW methane experiments with a door configuration and a low spark position.	39
Table 7. Measurements for the 37.5 kW methane experiments with a door configuration and a middle spark position.	40
Table 8. Measurements for the 37.5 kW methane experiments with a window configuration and a low spark position.	41
Table 9. Measurements for the 37.5 kW methane experiments with a window configuration and a middle spark position.	42
Table 10. Measurements for the 16.7 kW propane experiments with a door configuration and a low spark position.	43
Table 11. Measurements for the 16.7 kW propane experiments with a door configuration and a middle spark position.	44
Table 12. Measurements for the 16.7 kW propane experiments with a window configuration and a low spark position.	45
Table 13. Measurements for the 16.7 kW propane experiments with a window configuration and a middle spark position.	46
Table 14. Measurements for the 25.0 kW propane experiments with a door configuration and a low spark position.	47
Table 15. Measurements made for the 25.0 kW propane experiments with a door configuration and a middle spark position.....	48
Table 16. Measurements for the 25.0 kW propane experiments with a window configuration and a low spark position.	49
Table 17. Measurements made for the 25.0 kW propane experiments with a window configuration and a middle spark position.....	50
Table 18. Measurements for the 25.0 kW propene experiments with a door configuration and a low spark position.	51
Table 19. Measurements for the 25.0 kW propene experiments with a window configuration and a low spark position.	52
Table 20. Expected structural damage based on overpressures.	56
Table 21. Theoretical maximum deflection and maximum bending stress of the aluminum bars based on an internal pressure of 6.9 kPa (1 psi) and an extreme internal pressure of 34.5 kPa (5 psi).	59
Table 22. A range of steady-state interior compartment temperatures and the resulting theoretical exterior wall temperatures.....	61

List of Figures

Fig. 1. The compartment dimensions from the front side with the front door shown in a dashed border.	4
Fig. 2. The compartment dimensions from the top with the front door and the rear pressure relief panel shown.	4
Fig. 3. The cross-section of the composite wall showing the ceramic fiber board on the interior surface, ceramic fiber paper, aluminum sheet, and aluminum frame on the exterior. .	5
Fig. 4. The pressure relief panel is the rear wall of the compartment.	6
Fig. 5. A close pin holding the pressure relief panel closed, the lanyards attached to the ends of the pin to prevent the pin pieces from traveling if the pin breaks (left). Sheared pins after calibrating the door using a measuring scale (right).	6
Fig. 6. The open front door with two pneumatic arms.	7
Fig. 7. The composite cross-section of the front door with 2.5 cm ceramic board on the interior, 3 mm thick ceramic fiber paper, 6.4 mm aluminum sheet, and an aluminum frame on the exterior.	8
Fig. 8. The right wall circular vent with vertically sliding gate, exterior view (left), and interior view (right).	8
Fig. 9. The smaller window configuration with the metal plate placed inside the front door of the compartment represents a window opening.	9
Fig. 10. Compartment setup including gas fuel path to the burner within the reduced-scale compartment (HFG = Heat Flux Gauge, DAQ = Data Acquisition System). All measurements shown are nominal interior dimensions and the figure is not to scale.	10
Fig. 11. Gas fuel flowed through the MFC then up through the compartment floor into the bottom of the burner.	11
Fig. 12. The square gas burner positioned towards the rear of the compartment.	11
Fig. 13. The front sectional view of the compartment measurements with the sensors (Port = Gas Sampling Port, P = Pressure Transducer, HFG = Heat Flux Gauge, TC = Thermocouple, S = Spark Ignitor). All measurements shown are nominal interior dimensions in centimeters. Spark ignitor lengths were interchangeable.	12
Fig. 14. The top sectional view of the compartment measurements with the sensors (Port = Gas Sampling Port, P = Pressure Transducer, HFG = Heat Flux Gauge, TC = Thermocouple, S = Spark Ignitor). All measurements shown are nominal interior dimensions in centimeters.	13
Fig. 15. One spark ignitor probe extending 5.4 cm out from the interior wall of the compartment (grounding rod positioned above).	13
Fig. 16. The spark ignitor ports on the left exterior wall of the compartment with spark ignitors attached and electronics below the compartment (left) and the three spark ignitor ports with unattached spark ignitors aligned vertically on the right exterior wall of the compartment (right).	14
Fig. 17. The grounding connection on the lower right exterior for the spark ignitors.	14
Fig. 18. The four thermocouples on the interior left wall of the compartment (left) and the four vertical thermocouples on the interior right wall of the compartment (right).	15
Fig. 19. The four thermocouples on the exterior left wall of the compartment were positioned in a square pattern (left) and the four vertical thermocouples on the exterior right wall of the compartment (right).	15

Fig. 20. The thermocouple on the roof exterior (left) and the floor exterior of the compartment (right). 16

Fig. 21. The interior heat flux gauge positioned at the interior floor of the compartment (left) and from the bottom exterior of the compartment with water cooling tubing entering and exiting the gauge with the flow indicating pinwheel (right). 16

Fig. 22. The external heat flux gauge and video camera locations around the compartment with approximate distances (± 0.05 m). 17

Fig. 23. The opening on the left interior wall for the pressure measurement (left) and the pressure transducer attached to the left exterior wall of the compartment (right). 18

Fig. 24. The gas sampling ports set on the left interior (left) and left exterior compartment wall (right). 18

Fig. 25. The front-facing video camera field of view centered on the midpoint of the front door and with a lower boundary just below the digital clock on the shelf below the compartment (BSEE 244). 21

Fig. 26. Maximum vertical flame depth measurement from the top of the door from the front camera (BSEE 239). 21

Fig. 27. The left side facing video camera field of view with the red event light on the left border focused on the region outside the front door and a lower boundary just below the bottom edge of the compartment (BSEE 243). 22

Fig. 28. Horizontal flame extension measurement at the top of the door from the front face of the compartment out to the furthest flame front extension for the left camera (BSEE 239). . 22

Fig. 29. A representative 25.0 kW methane fire after ignition (top, BSEE 61), a non-event after the front opens (bottom left, BSEE 61), and maximum flame extension during a backdraft event (bottom right, BSEE 52). 24

Fig. 30. A representative 37.5 kW methane fire after ignition (top, BSEE 103), a non-event after the front opens (bottom left, BSEE 109), and maximum flame extension during a backdraft event (bottom right, BSEE 103). 25

Fig. 31. Pressure, heat flux, temperature measurements for a 25.0 kW methane fire. Note the temperature spikes at 480 s (450 s fuel time plus 30 s until the door opens) when the front opens for the backdraft event (red line) compared to the non-event (black dashed line) (non-event BSEE 61, event BSEE 52). Expanded uncertainties in the measurements were estimated from Type B evaluation of uncertainties to be 0.15 % for pressure, 3.0 % for heat flux, and 2.20 °C or 0.75 % (whichever is greater) for temperature. 26

Fig. 32. Pressure, heat flux, temperature measurements for a 37.5 kW methane fire. Note the temperature spikes at 330 s (300 s of fuel plus 30 s) after the front opens for the backdraft event (red line) compared to the non-event (black dashed line) (non-event BSEE 109, event BSEE 103). Expanded uncertainties in the measurements were estimated from Type B evaluation of uncertainties to be 0.15 % for pressure, 3.0 % for heat flux, and 2.20 °C or 0.75 % (whichever is greater) for temperature. 27

Fig. 33. A representative 16.7 kW propane fire after ignition (top, BSEE 203), a non-event after the front opens (bottom left, BSEE 203), and maximum flame extension during a backdraft event (bottom right, BSEE 191). 28

Fig. 34. A representative 25.0 kW propane fire after ignition (top, BSEE 132), a non-event after the front opens (bottom left, BSEE 132), and maximum flame extension during a backdraft event (bottom right, BSEE 167). 29

Fig. 35. Pressure, heat flux, temperature measurements for a 16.7 kW propane fire. Note the temperature spikes at 330 s (300 s of fuel plus 30 s) after the front opens for the backdraft event (red line) compared to the non-event (black dashed line) (non-event BSEE 213, event BSEE 197). Expanded uncertainties in the measurements were estimated from Type B evaluation of uncertainties to be 0.15 % for pressure, 3.0 % for heat flux, and 2.20 °C or 0.75 % (whichever is greater) for temperature. 30

Fig. 36. Pressure, heat flux, temperature measurements for a 25.0 kW propane fire. Note the temperature spikes at 330 s (300 s of fuel plus 30 s) after the front opens for the backdraft event (red line) compared to the non-event (black dashed line) (non-event BSEE 153, event BSEE 150). Expanded uncertainties in the measurements were estimated from Type B evaluation of uncertainties to be 0.15 % for pressure, 3.0 % for heat flux, and 2.20 °C or 0.75 % (whichever is greater) for temperature. 31

Fig. 37. A representative 25.0 kW propene fire after ignition (top, BSEE 222), a non-event after the front opens (bottom left, BSEE 222), and maximum flame extension during a backdraft event (bottom right, BSEE 226). Note the layering within the compartment in the top image where the top of the flame is within the dark upper layer. Also note the dark smoke from the compartment in the non-event image (bottom left). The flame extension is easily observed mixed with the smoke that pushed outward from within the compartment during a backdraft event (bottom right). 32

Fig. 38. Pressure, heat flux, temperature measurements for a 25.0 kW propene fire. Note the temperature spikes at 300 s (270 s of fuel plus 30 s) after the front opens for the backdraft event (red line) compared to the non-event (black dashed line) (non-event BSEE 221, event BSEE 237). Expanded uncertainties in the measurements were estimated from Type B evaluation of uncertainties to be 0.15 % for pressure, 3.0 % for heat flux, and 2.20 °C or 0.75 % (whichever is greater) for temperature. 33

Fig. 39. The one-dimensional plane composite wall for the compartment with the ceramic board as the interior layer of the enclosure and aluminum as the structural support. The heat source is on the inside of the enclosure. 60

1. Introduction

Backdraft and smoke explosions are extreme fire phenomena that can be deadly to firefighters and civilians [1-5]. Limited ventilation in any confined space can increase the likelihood of a backdraft event during a fire. Currently, observations on the fire ground are used to determine backdraft potential. Signs of an imminent backdraft include pressurized dark brown or black sooty smoke pushing or pulling ('puffing') out from the interior around vents and doors. Windows may also show evidence of high heat on their interior with brown stains and window glass cracks. These clues may not be obvious even to an experienced firefighter during an active fire scene. However, it may be possible to forecast backdraft potential by monitoring conditions within enclosed spaces.

In general, backdraft occurs when fresh air is introduced into a confined space where a high concentration of heated gas resides [6-9]. A room fire that is starved of oxygen limits its combustion rate and will reduce to a smoldering state but continues to generate heat and fuel vapors. When fresh air is rapidly introduced into the room through a large opening (e.g., door open or broken window) and mixes with the fuel vapors, an ignition may occur and lead to a backdraft [10]. Conversely, a flammable mixture existing in an enclosure that ignites is defined as a smoke explosion. NFPA 921 does not distinguish between backdrafts and smoke explosions and identifies them as the same phenomenon.

Initial backdraft experiments were conducted by Fleischmann [11] in a reduced-scale compartment to develop a basic understanding of the backdraft phenomenon. A 1.2 m x 1.2 m x 2.4 m compartment was built with two layers of gypsum wallboard attached to the interior of a steel frame designed to withstand an internal compartment pressure of 5 kPa. A bottom-hinged, single latched door 0.4 m x 1.1 m was on the opposite end from the 0.3 m x 0.3 m methane gas burner and overhead spark ignitor. One of the long walls was designed to be the pressure relief panel and was hinged to open if the internal pressure within the compartment was greater than 1 kPa. A small vent in the wall with the door was opened during the spark ignition of the burner to keep the initial pressure from spiking during ignition and causing the pressure relief panel to open. Gas concentrations of oxygen, carbon dioxide, carbon monoxide, and hydrocarbons were measured. A pressure transducer was used to measure the pressure differential between the inside and outside of the compartment. Thermocouples were also used to measure the inside temperatures. Two fuel flow rates were used, 70 kW and 200 kW. Results showed that the hydrocarbon concentration must be greater than 10 % for a backdraft to occur. Larger concentrations of hydrocarbons resulted in larger overpressures within the compartment. Temperatures within the compartment were less than 630 °C, and overpressures less than 258 Pa.

In order to obtain experimental data that would determine the effects of scaled compartment size compared to Fleischmann's reduced-scale compartment [11], a full-scale compartment was used to develop backdrafts [12]. The scaled size of the compartment was not determined to have a significant impact on the backdraft event, but the outside wind did impact the results. A shipping container was used for the full-scale compartment and was 2.2 m x 2.2 m x 5.4 m. The pressure relief panel was the short wall, 2.2 m x 2.2 m, and was calculated to have a static designed pressure of 0.92 kPa, with a maximum pressure not to exceed 1.92 kPa, sufficient based on the container strength, expected pressure, including the effect of wind. The pressure relief panel was opposite the wall with the front opening, 2.2 m x 0.8 m. Methane gas was used as the fuel for comparison to Fleischmann's 1994 study [11]. Internal compartment temperatures and pressures were measured. The estimated velocity of the vent

flow at the front opening was measured. A 0.3 m vent hole was kept open during ignition to prevent the pressure spike and closed after conditions stabilized. Oxygen, air, methane, and carbon dioxide were measured. The heat release rate for the tests ranged between 393 kW to 510 kW. Temperatures were roughly less than 680 °C. Pressures ranged from 6 Pa to 43 Pa with an average of 14 Pa.

Sutherland (1999) [13] studied smoke explosions by burning wood cribs using a reduced-scale compartment (1 m x 0.95 m x 1.48 m). The pressure relief panel (0.76 m x 0.76 m) was the compartment's floor with a spring latch set to open when the internal compartment pressure reached 2 kPa (0.3 psi). Two adjustable front openings were used, one opening high, the other low. Differential pressure and temperatures inside the compartment were measured. Carbon monoxide, carbon dioxide, oxygen, helium, and nitrogen were sampled. A medium-density fiber board was used as the fuel. Out of 11 experiments, a single smoke explosion was achieved from two experiments using a 4 kg wood crib, and two experiments using an 8 kg crib produced two smoke explosions each. All of these experiments had front entryway openings of 100 mm diameters. Their temperature and pressure measurements yielded a precondition environment within their compartment before combustion. Based on their results, the oxygen build-up in the upper layers within the compartment is most likely the trigger igniting the smoldering crib.

Weng and Fan (2003) [14] used a reduced-scale compartment 1.2 m x 0.6 m x 0.6 m with a methane burner to study parameters that may influence backdraft. Temperatures and differential compartment pressures were measured. Gas concentrations within the compartment were sampled, including oxygen, carbon dioxide, and carbon monoxide. Bidirectional probes measured flow through the front opening. They found that the critical parameter that predicts a backdraft is the mass fraction of unburned fuel, determined to be 9.8 %. Different opening geometries and locations were found to affect the occurrence of backdrafts, and water mist decreased backdraft flame expansion [15].

Chen (2012) [16] used a reduced-scale compartment (1.5 m x 1.2 m x 1.2 m) to study how vent size openings and fuel height affect smoke explosion events using wood fuel. Temperatures and pressures were measured at various locations. Combustion gases (i.e., CO, CO₂, and O₂) were sampled from various locations within the compartment. Chen found that the vent size had to be larger than 50 mm diameter for a smoke explosion to occur. The fuel height did not impact a smoke explosion but only affected the temperature profile inside the compartment.

Full-scale backdraft experiments were conducted by Gottuk et al. [17, 18] using a full-scale steel structure (2.44 m x 2.44 m x 4.88 m) with a single door opening using a diesel fuel spray. Backdraft mitigation was studied by introducing a water spray into the heated compartment before the door was opened. The experiments were conducted outdoors. The wind was considered but determined to be an uncontrollable factor in their experiments. The maximum overpressures observed in backdrafts were 100 Pa to 280 Pa. Typical compartment temperatures were 340 °C to 420 °C when the door was opened. When a fireball was observed to exit the room's front door, it usually occurred within 20 s of the door opening. Fireballs were observed to extend 9 m from the doorway and were up to 7 m in diameter. A minimum diesel fuel concentration of 16 % by mass was a key parameter needed to initiate a diesel backdraft explosion. The water spray's primary effect of reducing the backdraft explosion was by diluting, rather than cooling, the atmosphere within the room.

Gojkovic (2001) [19] conducted methane-fueled backdraft experiments in a full-scale container (5 m x 2 m x 2 m) with a pressure relief panel along one short end of the container.

The pressure relief panel was held by plastic wires that released the panel if unwanted overpressure developed to avoid damaging the container. A rectangular opening at the front served as the front door or window to allow fresh air into the compartment during testing. A heated wire was used to provide the ignition to the fuel-air mixture. Pressure during testing measured less than 250 Pa. Temperatures within the container increased as long as enough oxygen was available. Once the oxygen was depleted, the temperature started to lower and then continued to lower when the front opening opened and fresh air entered. Once the mixture ignited, the temperature peaked. Pressure also peaked during the backdraft, followed by a slight under pressure.

Tsai and Chiu (2013) [20] conducted full-scale backdraft experiments using polyurethane foam furniture as solid fuel in a steel storage container 5.9 m x 2.35 m x 2.4 m. Six thermocouple trees with 10 Type-K thermocouples each were used to measure temperature. A paramagnetic oxygen analyzer measured the oxygen concentration during the tests. A thermal imager was used to measure the flame temperature during their experiments. Typically, a backdraft event occurred about 30 s to 50 s after fresh air was introduced by opening the container. Flammable wall materials were necessary to initiate a backdraft event.

This report documents a 2/5th scale compartment utilized to expeditiously conduct multiple backdraft experiments in a safe and controlled environment. The purpose of these experiments was to determine if compartment monitoring can provide information that indicates a potential backdraft. Establishing backdraft indicators would improve firefighters' situational awareness and mitigate substantial risk at fire scenes.

2. Methods

2.1. The Reduced-Scale Compartment

The reduced-scale compartment (RSC) was designed to be a 2/5ths scale replicate of the ISO/ASTM standard full-scale test room (2.44 m x 2.44 m x 3.66 m) [21, 22]. The nominal internal dimensions of the compartment were 99 cm (wide) x 99 cm (high) x 152 cm (long) (Fig. 1 and Fig. 2)¹.

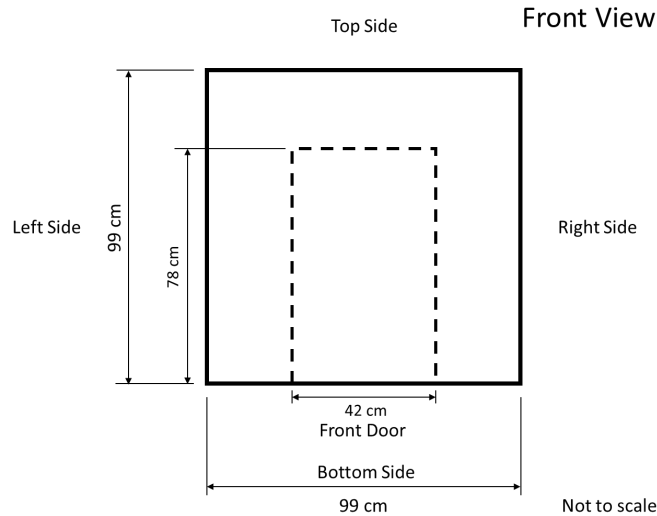


Fig. 1. The compartment dimensions from the front side with the front door shown in a dashed border.

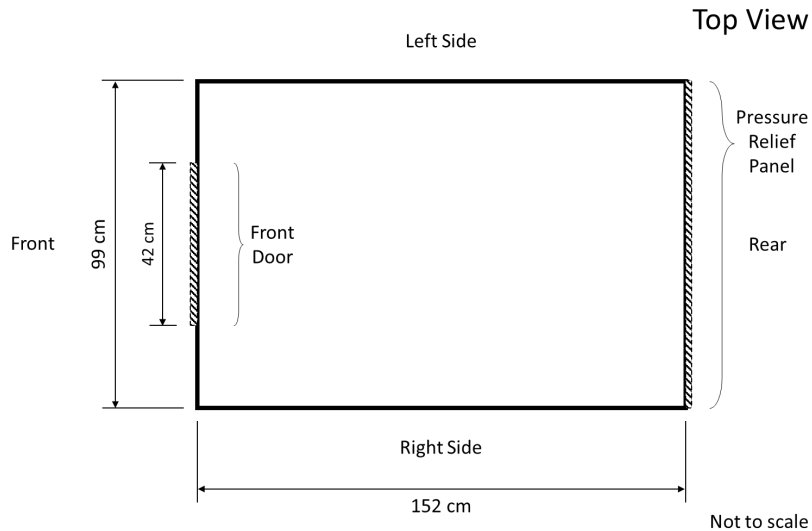


Fig. 2. The compartment dimensions from the top with the front door and the rear pressure relief panel shown.

¹ All compartment and related dimensions are nominal values.

The RSC was built to withstand anticipated high temperatures and overpressure within the compartment during repeated backdraft experiments. A composite wall was constructed on all sides of the compartment (Fig. 3). The interior surface of the compartment was 2.5 cm high-temperature ceramic fiber board (300 kg/m³, 1260 °C), thermal conductivity ≤ 0.153 W/(m·K)) to resist elevated temperatures and protect the structural components. The exterior surface of the ceramic board was lined with 3 mm thick high-temperature insulation ceramic fiber paper to seal the seams between the ceramic board.

The last layer of the composite wall was a 9.5 mm thick aluminum sheet to which the ceramic board and fiber paper were fastened. The aluminum sheet was fastened to an aluminum frame that together provided structural support.

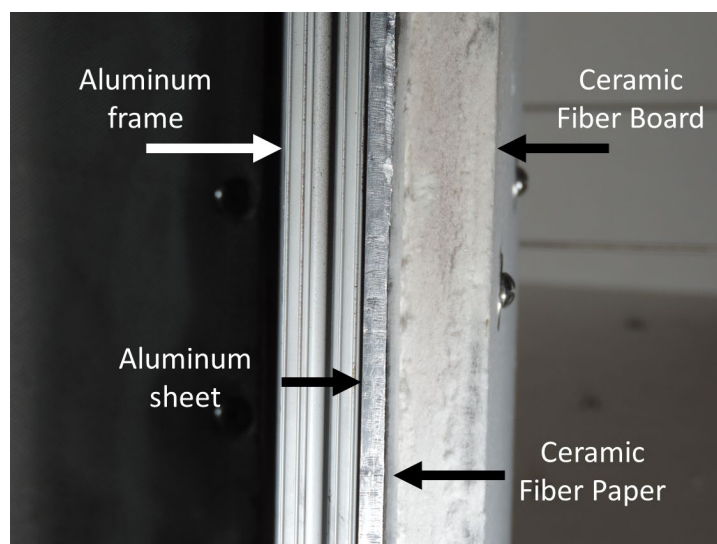


Fig. 3. The cross-section of the composite wall showing the ceramic fiber board on the interior surface, ceramic fiber paper, aluminum sheet, and aluminum frame on the exterior.

Calculations were performed to show that the structural aluminum frame of the compartment can withstand the bending stress and deflections due to internal pressures that the compartment may experience (Appendix A). Temperatures on the exterior of the compartment, at the aluminum frame, were expected to be less than 100 °C (Appendix A), below the temperatures expected to damage the structural aluminum under maximum designed overpressure.

2.2. Pressure Relief Panel

The primary hazards of concern beyond routine compartment fire experiments were the potential compartment overpressures experienced during backdrafts. The design goal of the compartment's pressure relief system was to mitigate excessive overpressures (> 0.7 kPa (0.1 psi)) during events that could pose a safety hazard or damage the compartment. This goal was achieved by implementing a pressure relief panel to mitigate the risk of overpressure within the compartment. Furthermore, the panel would allow the compartment to maintain its integrity without deforming during experiments.

The pressure relief panel was implemented at the compartment's rear, acting as its rear wall (Fig. 2 and Fig. 4). The pressure relief panel was constructed similarly to the compartment

walls with a 2.5 cm interior surface of ceramic fiber board, then 3.2 mm fiber paper, attached to a sheet of aluminum (Fig. 3). The aluminum wall thickness for the pressure relief panel was 3.2 mm, thinner than the other compartment aluminum walls, lowering the inertia of the panel. The aluminum sheet was fastened to a similar aluminum beam frame as with the other compartment walls.

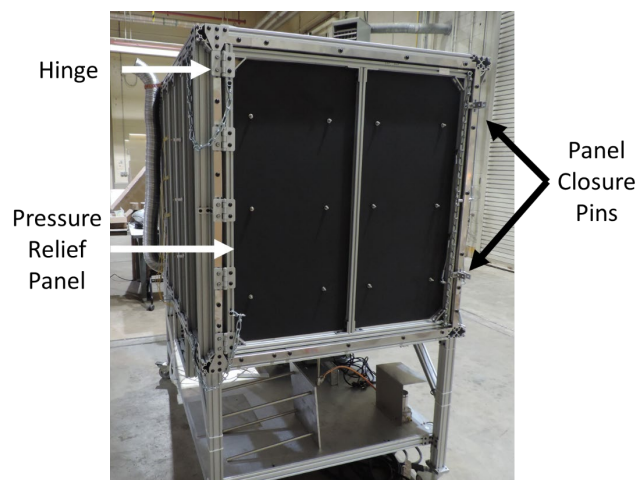


Fig. 4. The pressure relief panel is the rear wall of the compartment.

Two aluminum panel closure pins, approximately 5.7 cm long, with a 6 mm diameter, were used when the pressure relief panel was closed. A dog-bone shape was machined by milling the gauge section of the pins (1/4-20 in (6.4 mm) fastener) to a length of 1 cm. The final thickness of the ‘gauge section’ was 2 mm. The dimensions of the panel closure pins were chosen so that approximately 360 N shears the pins and opens the pressure relief panel, which occurs when the internal pressure reaches 0.7 kPa (0.1 psi). The 0.7 kPa (0.1 psi) overpressure was the maximum safe internal pressure for the compartment (Appendix A). Lanyards were fastened to either end of each pin to keep the pin parts from traveling if shearing occurs and the panel opens (Fig. 5).

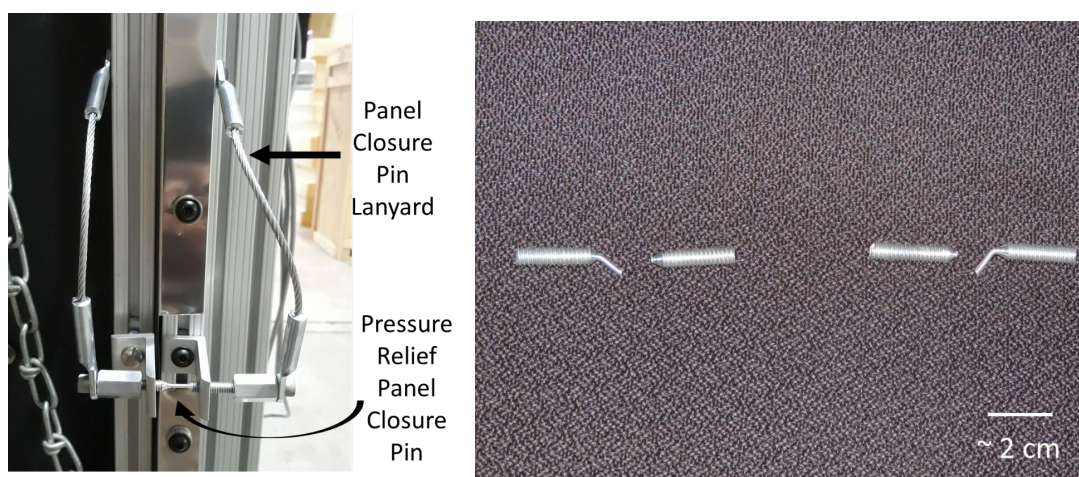


Fig. 5. A close pin holding the pressure relief panel closed, the lanyards attached to the ends of the pin to prevent the pin pieces from traveling if the pin breaks (left). Sheared pins after calibrating the door using a measuring scale (right).

2.3. Front Door and Window Configuration

The front door was centered horizontally in the front wall of the compartment (Fig. 6). In order to remain consistent with the 2/5ths scale reduced size for the compartment compared to the standardized test room, the front door interior dimensions were 42 cm wide and 78 cm tall (Fig. 1 and Fig. 2). These dimensions were comparable to Bryner et al. (1994) [23] and Bundy et al. (2007) [24], whose front door dimensions were 48 cm wide by 81 cm tall.



Fig. 6. The open front door with two pneumatic arms.

The composite front door thickness included a 2.5 cm ceramic board on the interior surface, a 3 mm thick ceramic fiber paper layer, and a 6.4 mm thick black-painted aluminum sheet fastened to the exterior aluminum frame. The front door construction was the same as the other compartment walls except that the aluminum sheet for the door was 6.4 mm instead of 9.5 mm. A cross-section of the door is shown in Fig. 7.

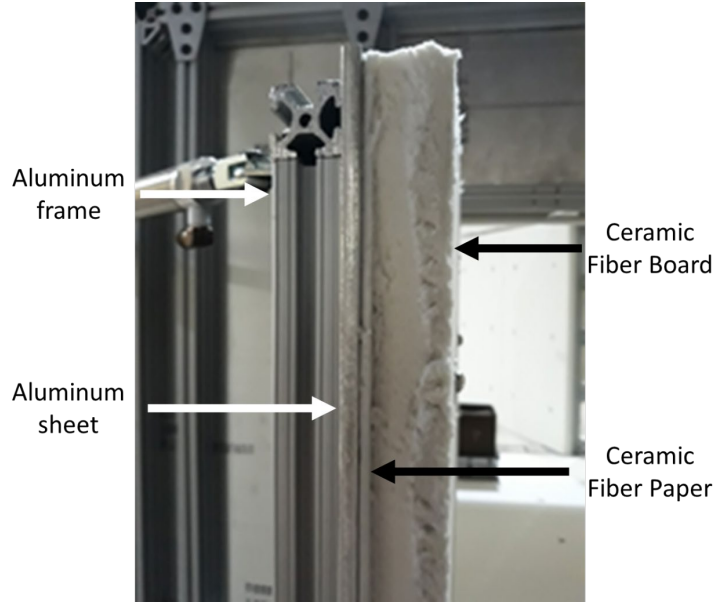


Fig. 7. The composite cross-section of the front door with 2.5 cm ceramic board on the interior, 3 mm thick ceramic fiber paper, 6.4 mm aluminum sheet, and an aluminum frame on the exterior.

A small circular vent with a 3.8 cm diameter was located in the lower right wall of the compartment, 38 cm from the front interior wall of the compartment and 3 cm above the compartment floor (Fig. 8). This vent produced a uniform leakage area when the door was closed. If the front door was closed, the vent was open, and the vent was closed when the front door was open. On the exterior of the right wall, a metal vent chute channeled the hot gas from the interior, away from the compartment. The vent gate slides vertically over the vent opening on the exterior of the wall.

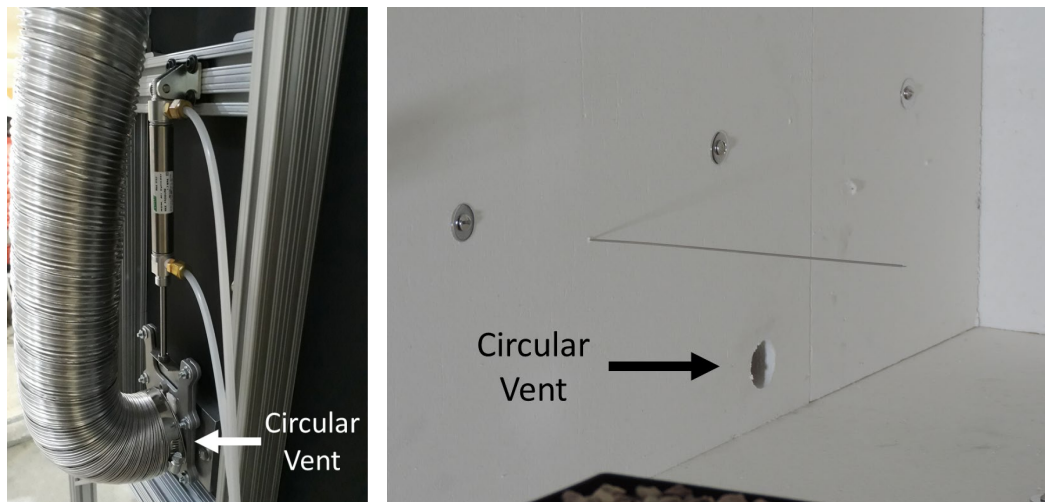


Fig. 8. The right wall circular vent with vertically sliding gate, exterior view (left), and interior view (right).

The front door was modified into the smaller window configuration by placing a 15 cm high metal plate inside the front door resting on the floor of the compartment (Fig. 9). The metal plate reduced the height of the front door from 78 cm to 63 cm.

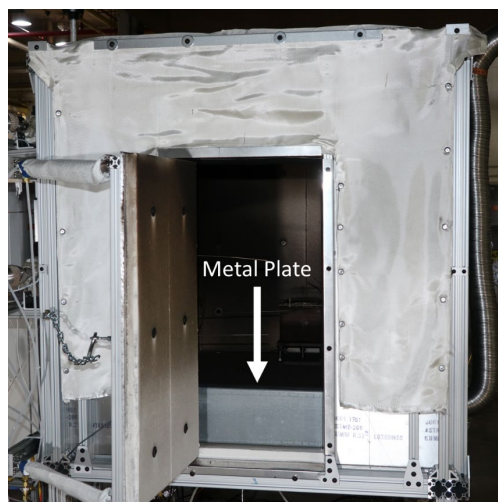


Fig. 9. The smaller window configuration with the metal plate placed inside the front door of the compartment represents a window opening.

2.4. Gas Fuel System

Fig. 10 displays the experimental setup that utilizes the constructed compartment to investigate backdrafts. Three gaseous fuels were used in these experiments: methane, propane, and propene. The fuel flow rate to the burner was controlled via a mass flow controller (MFC). Gas fuel was piped from the MFC to the burner through the compartment floor (Fig. 10 and 11). The fuel flow rate expanded uncertainty was estimated from the Type B evaluation of uncertainty to be 0.8 % of reading + 0.2 % of full scale².

² Unless otherwise stated, uncertainty in this manuscript is expressed as the expanded uncertainty with a coverage factor of 2, representing a 95% confidence level.

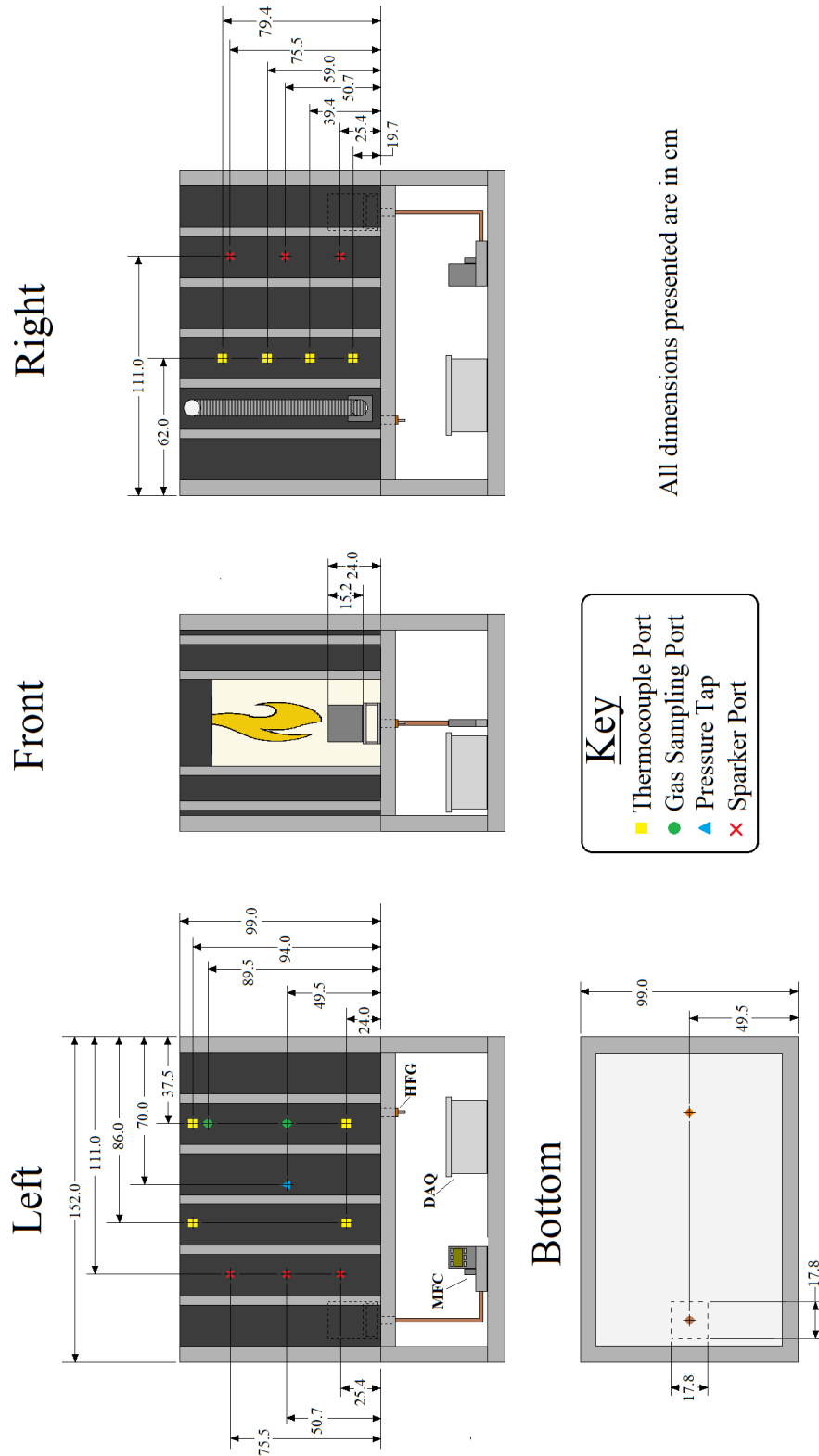


Fig. 10. Compartment setup including gas fuel path to the burner within the reduced-scale compartment (HFG = Heat Flux Gauge, DAQ = Data Acquisition System). All measurements shown are nominal interior dimensions and the figure is not to scale.

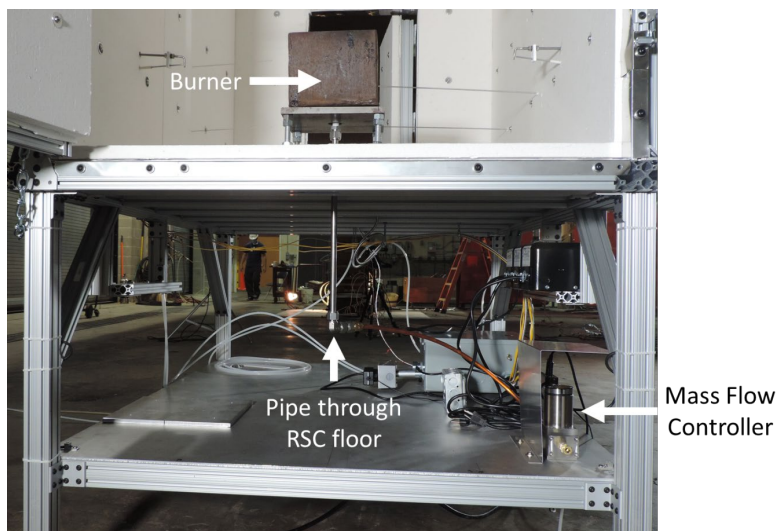


Fig. 11. Gas fuel flowed through the MFC then up through the compartment floor into the bottom of the burner.

A 17.8 cm square gas burner with a wall thickness of 3.2 mm, and a depth of 15.2 cm was positioned towards the rear of the compartment filled with stone (pea pebbles) (Fig. 12). The gas fuel pipe supplied gas to the burner and was located 21 cm from the rear interior wall and centered midway between the left and right sides (Fig. 14). The top of the burner was 24 cm above the compartment floor.

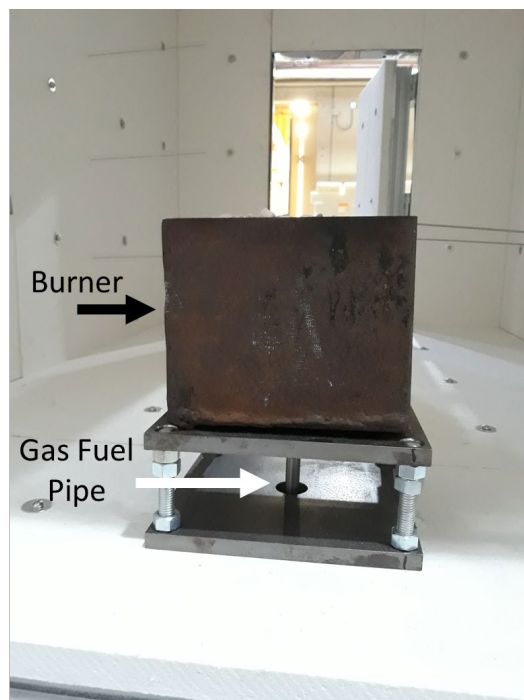


Fig. 12. The square gas burner positioned towards the rear of the compartment.

2.5. Spark Ignitors

Six spark ignitor ports were located along the sides of the compartment, three ports on the left wall and three on the right wall, to allow flexibility with the spark ignitor lengths and locations (Fig. 13 and Fig. 14). The interchangeable spark probes extended from the wall above the burner with three possible lengths: 10.8 cm, 25.4 cm, and 55.9 cm (Fig. 15). The lowest spark ignitor port was 25.4 cm from the floor. The middle spark ignitor port was located 50.7 cm from the compartment floor. The high spark ignitor port was located 75.5 cm from the compartment floor. The spark ports on both sides were located 111 cm from the interior front wall of the compartment.

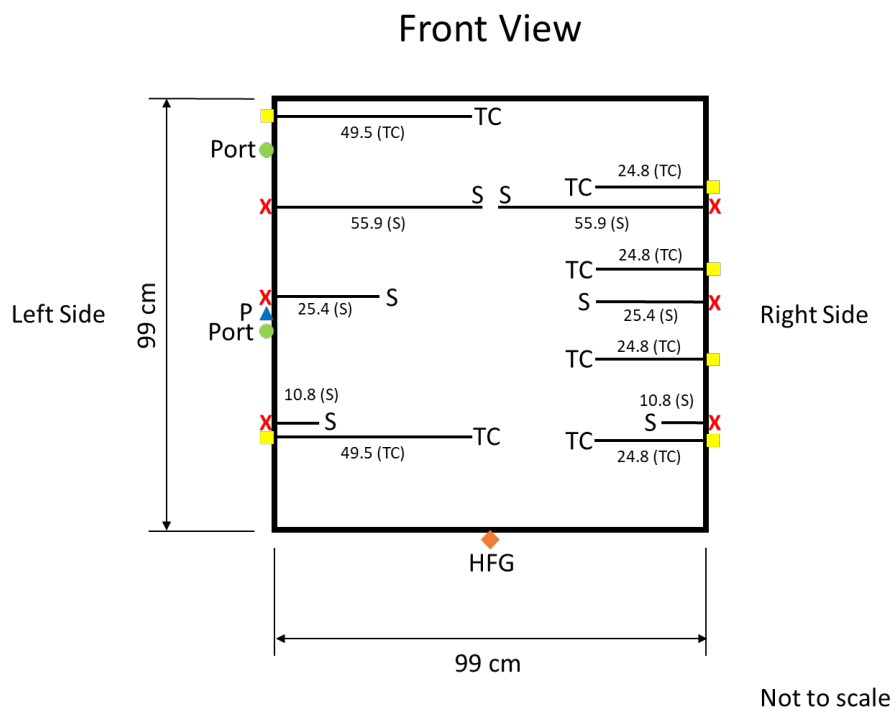


Fig. 13. The front sectional view of the compartment measurements with the sensors (Port = Gas Sampling Port, P = Pressure Transducer, HFG = Heat Flux Gauge, TC = Thermocouple, S = Spark Ignitor). All measurements shown are nominal interior dimensions in centimeters. Spark ignitor lengths were interchangeable.

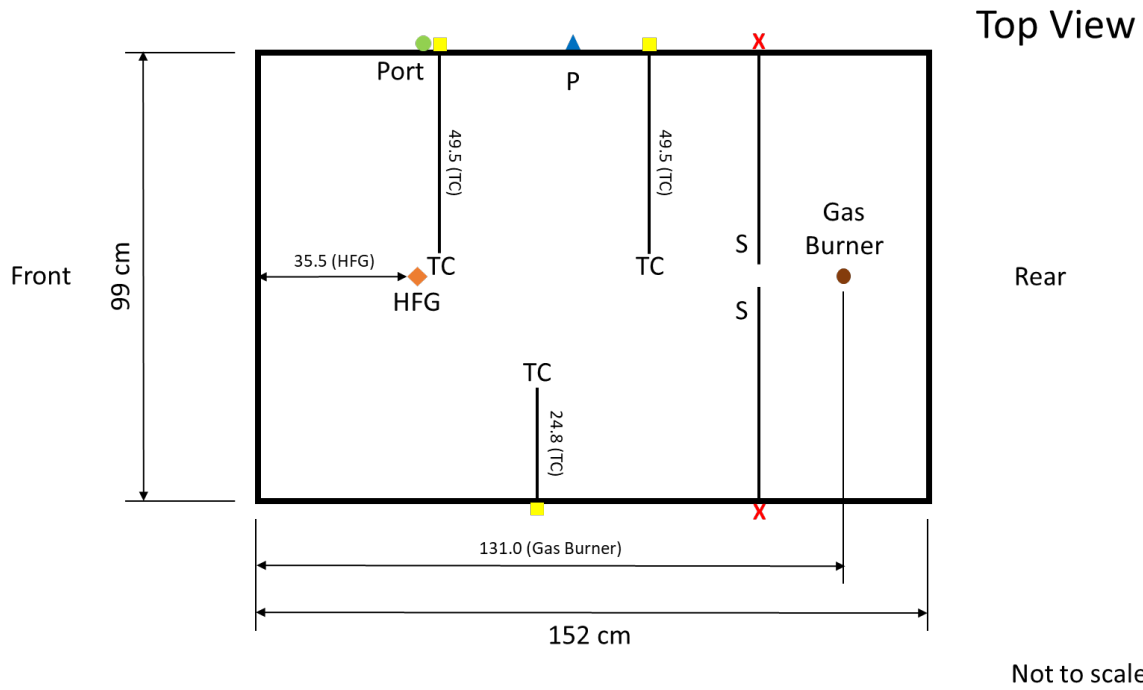


Fig. 14. The top sectional view of the compartment measurements with the sensors (Port = Gas Sampling Port, P = Pressure Transducer, HFG = Heat Flux Gauge, TC = Thermocouple, S = Spark Ignitor). All measurements shown are nominal interior dimensions in centimeters.

The voltage was supplied to create an electrical arc between the pair of probes (approximately 2 mm spark gap) (Fig. 15) using a spark ignitor (type LaX R6086, 120 V at 60 Hz) that attached to the exterior port on the compartment wall (Fig. 16). A ground connection was attached to both sides of the compartment panels (Fig. 17).



Fig. 15. One spark ignitor probe extending 5.4 cm out from the interior wall of the compartment (grounding rod positioned above).



Fig. 16. The spark ignitor ports on the left exterior wall of the compartment with spark ignitors attached and electronics below the compartment (left) and the three spark ignitor ports with unattached spark ignitors aligned vertically on the right exterior wall of the compartment (right).



Fig. 17. The grounding connection on the lower right exterior for the spark ignitors.

A red event light attached to the exterior of the compartment was triggered 20 s before a potential backdraft event. More specifically, the event light was used to alert the test space that the door would open in 20 s and a backdraft event was imminent. The event light also helped synchronize the video cameras.

2.6. Thermocouples

Thermocouples were positioned at various locations on the inside and exterior surfaces of the compartment (Fig. 13 and Fig. 14). The right side of the compartment had four sheathed 1.57 mm nominal diameter Type K copper-nickel thermocouples (Omega, HGKMQSS-062E-12), with a Type B evaluation of expanded uncertainty of 2.20 °C or 0.75 % (whichever is greater), oriented in line vertically and extended 24.8 cm from the interior wall (Fig. 18 and Fig. 19), and located 62 cm from the front interior wall. The lowest thermocouple was 19.7 cm

from the floor, the second thermocouple was 39.4 cm, the third thermocouple was 59 cm, and the fourth thermocouple was 79.4 cm from the compartment floor.

The left side of the compartment had four sheathed 3.2 mm nominal diameter Type K mineral-insulated thermocouples (Omega, KQXL-18U-24-CAL-3), with a Type B evaluation of expanded uncertainty of 2.20 °C or 0.75 % (whichever is greater), oriented in a box pattern that extended 49.5 cm from the interior wall (Fig. 18 and Fig. 19). The lower pair of thermocouples was located 24 cm above the compartment floor. The upper pair of thermocouples was located 5 cm from the compartment roof. The front pair was located 38 cm and the rear pair was located 86 cm from the front interior wall of the compartment.

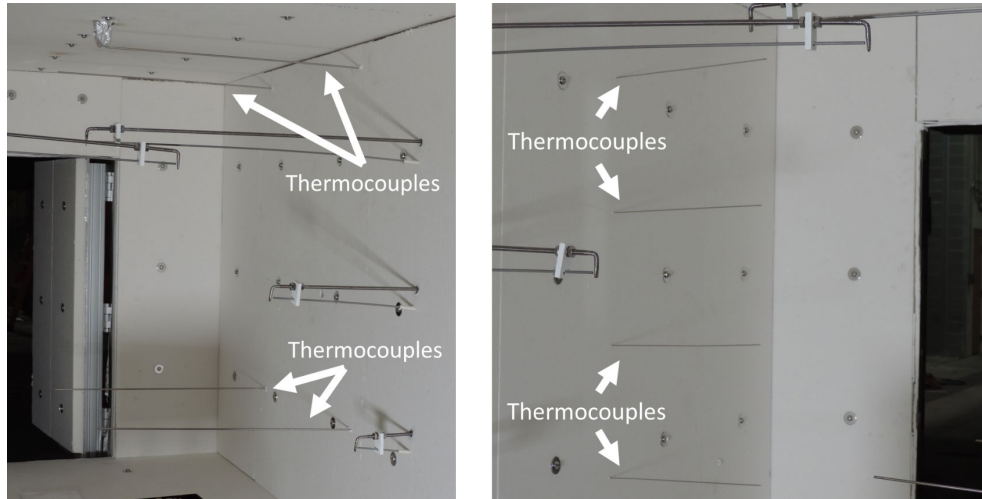


Fig. 18. The four thermocouples on the interior left wall of the compartment (left) and the four vertical thermocouples on the interior right wall of the compartment (right).

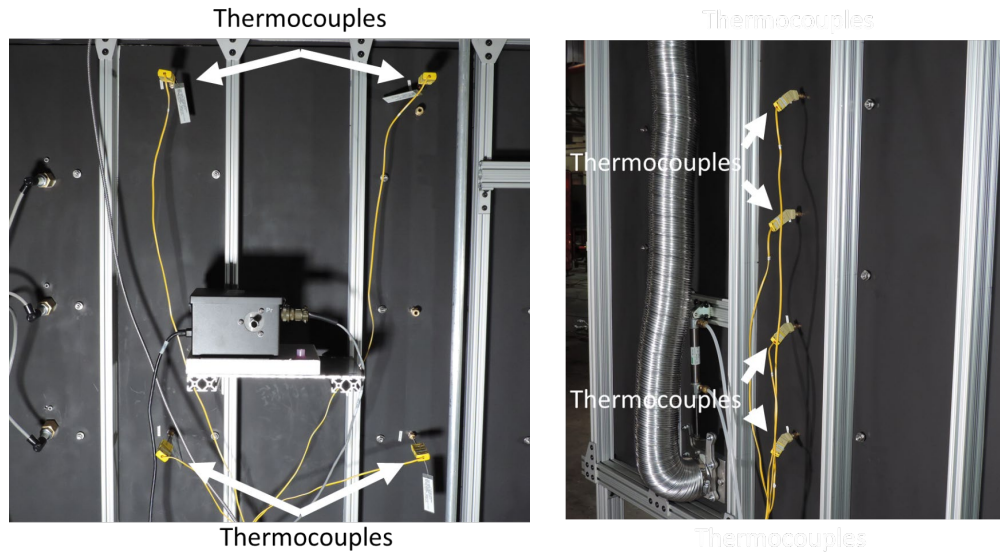


Fig. 19. The four thermocouples on the exterior left wall of the compartment were positioned in a square pattern (left) and the four vertical thermocouples on the exterior right wall of the compartment (right).

Two thermocouples (Omega WTK-HD-72-S) were used to measure temperature on the exterior surface of the compartment. The thermocouples were centered midway between the left and right sides of the compartment positioned at the top and bottom exterior. The thermocouple on the roof exterior was approximately 46.4 cm, and the thermocouple on the floor exterior was approximately 69.2 cm from the rear of the compartment. The exterior surface thermocouple measurements had a Type B evaluation of expanded uncertainty of 2.20 °C or 0.75 % (whichever is greater) (Fig. 20).

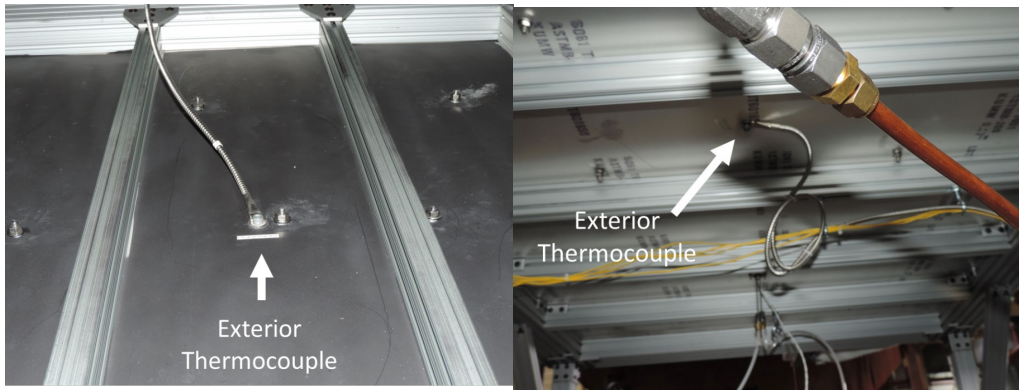


Fig. 20. The thermocouple on the roof exterior (left) and the floor exterior of the compartment (right).

2.7. Heat Flux Gauge

A water-cooled heat flux gauge (Medtherm 64-20FSB-20T) was located on the compartment's floor (Fig. 21), with a Type B evaluation of expanded uncertainty of 3.0 % of the reading. The interior heat flux gauge was centered horizontally 49.5 cm from either side wall (Fig. 13) and 35.5 cm (Fig. 14) from the interior front wall of the compartment. The cooling water flowed to the gauge from below the compartment floor (Fig. 21). Due to the importance of maintaining the cooling water flowing to the gauge, a pinwheel flow indicator was attached to the side of the compartment frame.

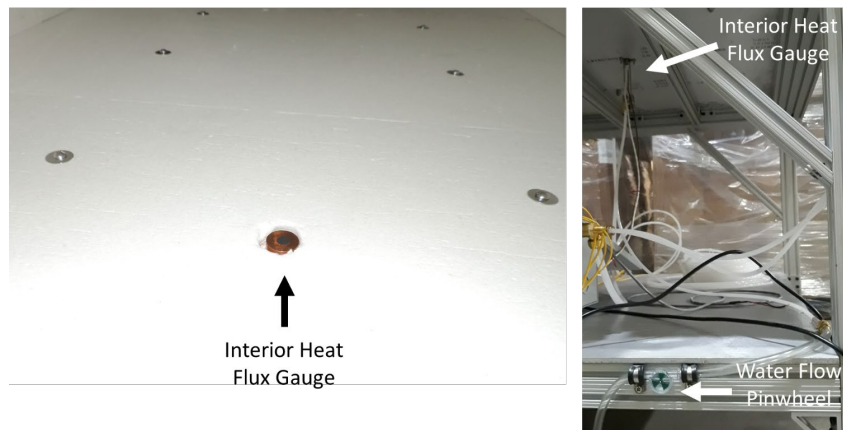


Fig. 21. The interior heat flux gauge positioned at the interior floor of the compartment (left) and from the bottom exterior of the compartment with water cooling tubing entering and exiting the gauge with the flow indicating pinwheel (right).

An additional heat flux gauge was implemented outside the compartment (Fig. 22) and was included after backdraft experiment (BSEE) 40. The exterior gauge was used to evaluate the heat flux exiting the compartment during a backdraft event. The gauge was located 4.6 m in front of the compartment and elevated 1.98 m from the facility floor. The expanded uncertainty of the external heat flux gauge measurements was estimated from the Type B evaluation of uncertainty to be 3.0 % of the reading.

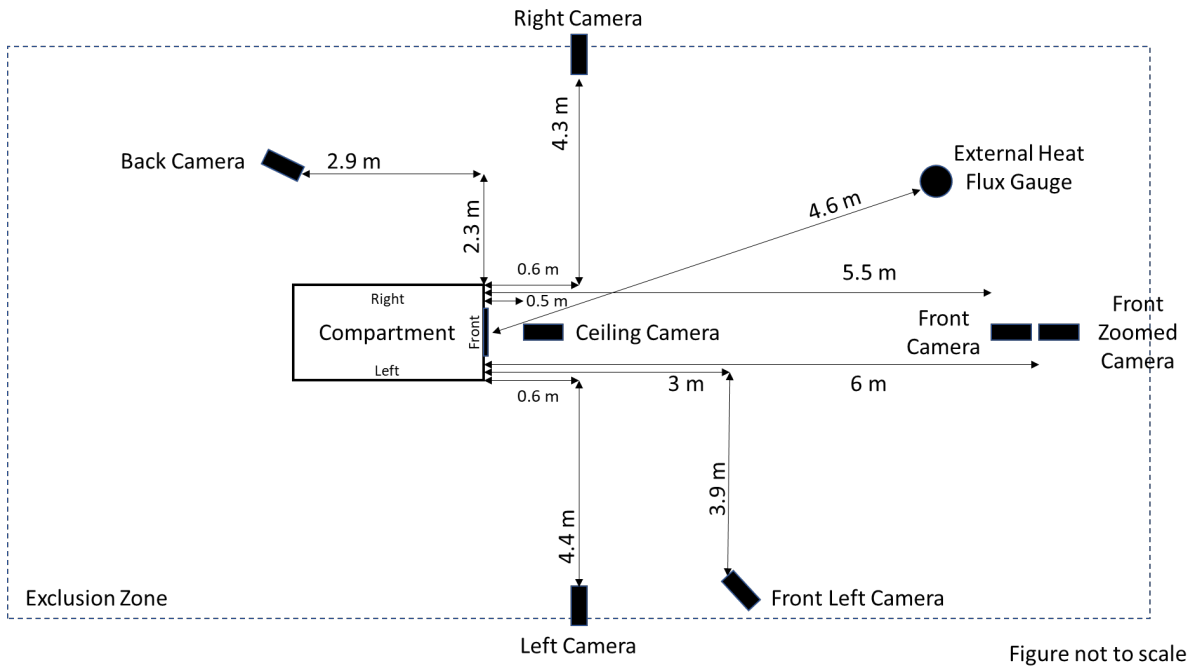


Fig. 22. The external heat flux gauge and video camera locations around the compartment with approximate distances (± 0.05 m).

2.8. Pressure Transducer

A differential pressure transducer (MKS Type 220DD) was used to compare the pressure inside the compartment to the ambient pressure outside the compartment (Fig. 23). The transducer was positioned in the left interior wall and centered vertically, 49.5 cm above the interior floor of the compartment (Fig. 13) and was 70 cm from the front interior of the compartment (Fig. 14). The expanded uncertainty of the pressure transducer measurements was estimated from the Type B evaluation of uncertainty to be 0.15 % of reading.

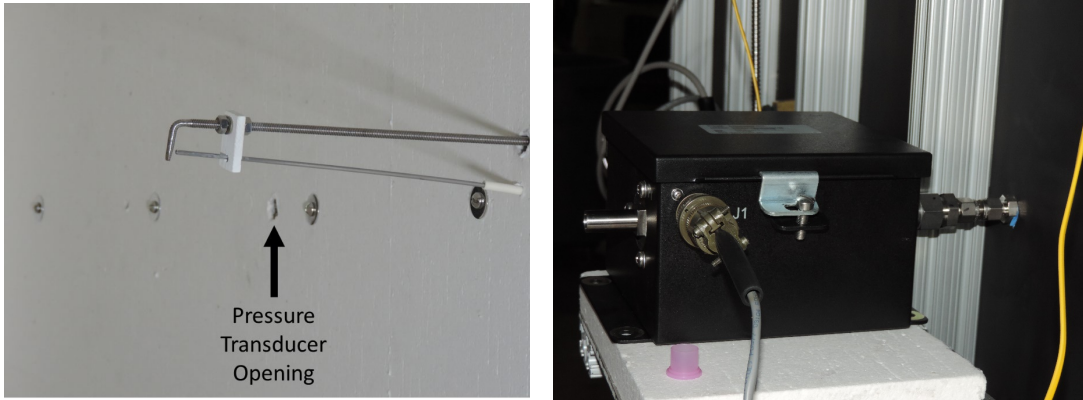


Fig. 23. The opening on the left interior wall for the pressure measurement (left) and the pressure transducer attached to the left exterior wall of the compartment (right).

2.9. Gas Sampling

Two gas sampling ports were located on the left wall aligned vertically, 37.5 cm (Fig. 24) from the front interior wall of the compartment (Fig. 14). The lower port was 50 cm, and the upper port was 89.5 cm above the interior floor (Fig. 13). Stainless steel, thin-walled tubes (outer diameter 0.6 cm) extended 49.5 cm into the compartment attached to these two ports and extracted gas samples throughout the experiments. Gas sampling results will be presented in a future report.

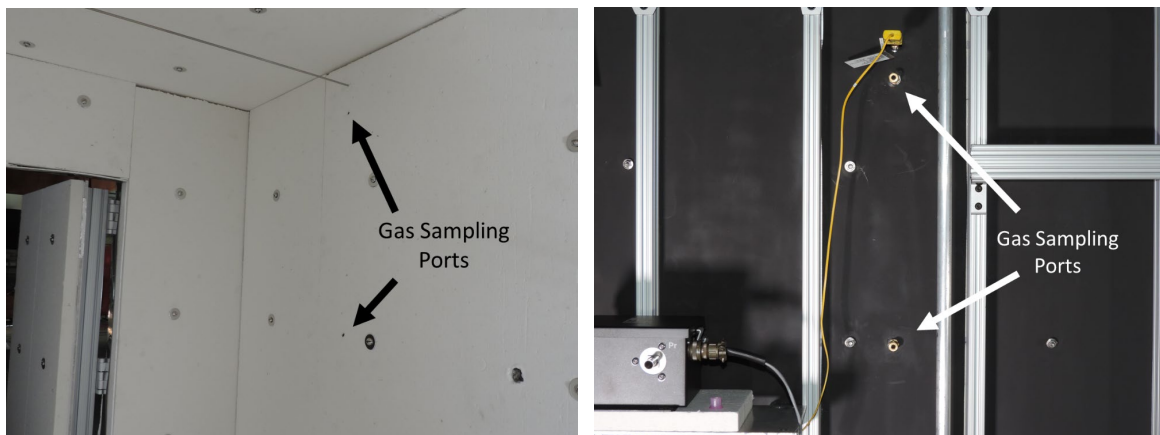


Fig. 24. The gas sampling ports set on the left interior (left) and left exterior compartment wall (right).

2.10. Data Acquisition System

Data were obtained via a data acquisition system (DAQ) controlled by LabVIEW. The sampling rate varied throughout the experiment. For most of the experiment, the DAQ sampled data at 1 Hz. The sampling rate was maintained at approximately 25 Hz 40 s prior to and 20 s after the door opening. The sampling rate change was triggered via LabVIEW code and implemented to resolve rapidly fluctuating heat flux and pressure values. The DAQ also

prompted specified equipment during the experiment, including the front door, spark ignitors, and red event light.

2.11. General Experiment Procedure

Experiments followed a general process divided into three major events: 1) background conditions; 2) prior to anticipated backdraft event; 3) anticipated backdraft event.

- 1) **Background Conditions:** Prior to burner ignition, variable compartment configurations, including fuel type, fire size, fuel-off time, compartment opening configuration, spark position, and spark delay time, were determined and adjusted accordingly. Methane, propane, and propene were chosen as the fuels of interest. The fire size ranged from 16.7 kW to 37.5 kW utilizing various fuels. A 25 kW fire size was studied using each fuel to compare outcomes across a wide fuel range. Fuel-off time was defined as the duration of gaseous fuel flow into the compartment from the time of ignition. Compartment opening configuration included a door and window opening as described in Section 2.3. Spark position encompassed the sparkers at either the low or middle positions as detailed in Section 2.5.

After the compartment configuration was set, background data was collected using the DAQ for all instruments and video cameras for one minute (Table 1). Once background data was recorded, a gas torch was used to ignite a small 6 kW fire at the burner inside the compartment. Once the burner ignited, the target fire size was scaled up to a predetermined value where it then steadily burned while the front door was open for 60 s.

- 2) **Prior to Anticipated Backdraft Event:** After the front door was closed, fuel was continuously fed to the burner for the predetermined amount of time, after which the MFC was set to 0 standard liters per minute (SLPM). The red event light was prompted 10 s after shutting off the fuel line to indicate to observers that the door would open in 20 s.
- 3) **Anticipated Backdraft Event:** The door opened 30 s after shutting off the fuel line, at which time the spark ignitors were armed. In some instances, the spark ignitors were delayed 5 s from when the door opened. The opened door allowed ambient air to be drawn into the compartment and mix with the fuel present.

Upon opening the doorway of the compartment during the anticipated backdraft event, five different scenarios were observed to occur: 1) no ignition occurred, and the hot gas and smoke exited the compartment; 2) a flame was observed to still reside at the burner, and no backdraft was achieved; 3) a local ignition briefly occurred with the combustion contained within a small region of the compartment; 4) an ignition occurred at the ignitor with the combustion expanding throughout the majority of the compartment and transitioning to the exterior, slightly extending beyond the doorway; 5) an ignition occurred at the ignitor with the combustion expanding throughout the compartment, and vastly extending beyond the doorway signifying a backdraft.

Table 1. Timeline of critical experiment occurrences.

Major Event	Time	Occurrence
Background Conditions	Prior to Ignition	Background data collected, door open
Prior to Anticipated Backdraft	0	Manual ignition, 6 kW fire size, door open
	0 s to 20 s	6 kW ramped up to predetermined fire size, door open
	20 s to 60 s	Fire steadily burns in the compartment with door open
	60 s	Door closed
	60 s to Fuel-off time	Continuous fuel flow to burner, door closed
	Fuel-off time	Fuel flow to burner set to 0 SLPM, door closed
	Fuel-off time + 10 s	Red event light is on, door closed
Anticipated Backdraft	Fuel-off time + 30 s	Door open
	Fuel-off time + 30 s + spark delay	Spark ignited (after 0 or 5 s delay), door open, potential event

2.12. Video Measurements of Backdraft Geometry

Seven exterior video cameras (Canon VIXIA HF800) were used to record each experiment from various locations around the compartment (Fig. 22). All cameras were focused manually and had a UV light lens to help protect the camera lens from damage and debris. Video recording was manually started and stopped at each camera before and after each experiment. Individual frames of the video recordings were used to estimate the time of events and dimensions of flames for a backdraft event in a post hoc analysis. Individual video frames were obtained by processing video recordings via OpenShot Video Editor and VLC Media Player and primarily included a backdraft event of which the flame had exited the compartment. Distances were measured using an object of known length within the image of interest. For a single image, distance measurements were taken at least twice.

The front camera was used to determine the ignition time. The ignition time was defined as the difference between when the front door began to open and when ignition was observed within the compartment. The front camera was also used to estimate the maximum vertical depth of flame extension. The front camera faced the front of the compartment in line with the vertical midpoint of the front door (Fig. 25). The camera was 5.5 m from the front exterior compartment face, and the front lens was elevated 122 cm above the floor³. The camera's view focused on the region outside the front door, capturing just below the digital clock on the

³ Camera positions are approximate distances.

bottom shelf and several feet above the compartment top. As displayed in Fig. 26, the maximum vertical depth of flame extension was measured down from the top of the compartment door and reported as a percentage of the front door opening.

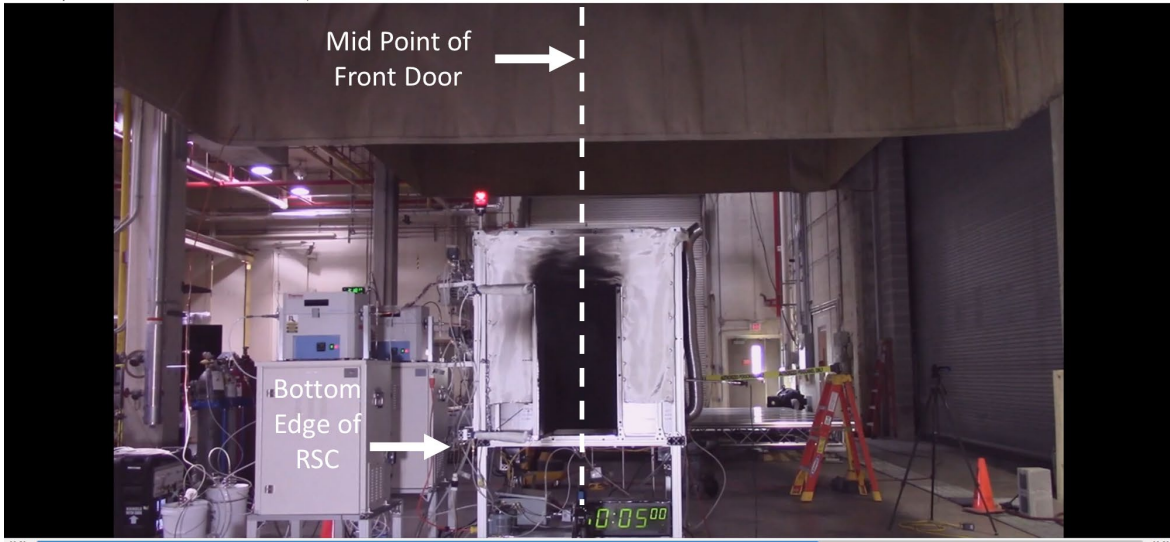


Fig. 25. The front-facing video camera field of view centered on the midpoint of the front door and with a lower boundary just below the digital clock on the shelf below the compartment (BSEE 244).



Fig. 26. Maximum vertical flame depth measurement from the top of the door from the front camera (BSEE 239).

The left camera was used to estimate the maximum flame extension horizontally from the top of the front door. Only the left camera was used for this measurement because the leading edge of the flame was easier to measure against the dark background in the left camera images. The left video camera was positioned to face the left side of the compartment, 4.4 m from the left exterior compartment wall (Fig. 22), and the front lens was elevated 122 cm above the floor. The camera was also offset 0.6 m such that the center of the camera view was focused

on the region outside the open front compartment door (Fig. 27). The camera view was framed from the red event light at the top of the compartment to its bottom edge.

The horizontal flame extension was measured from the front face of the compartment to the maximum flame extension at the top of the compartment door (Fig. 28). An image of a ruler in the same field of view as the flame extension was used to scale and acquire a length measurement reported in meters. The uncertainty of the dimensions was determined from the Type B evaluation of uncertainty. The bias error source was estimated from the distance marker and the maximum extension on a centerline (approx. 5 cm), assuming minimal parallax.

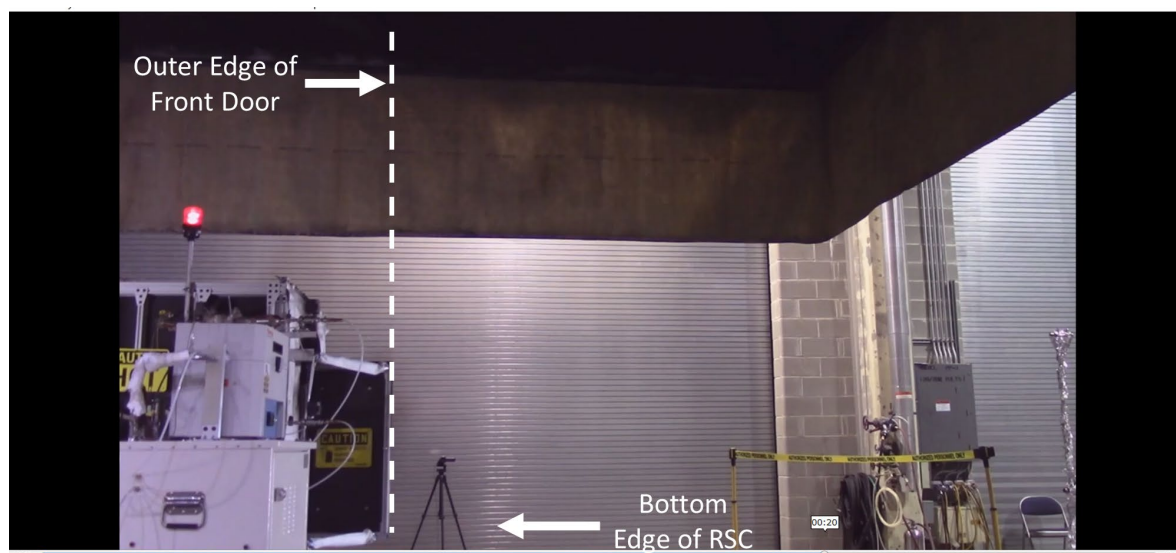


Fig. 27. The left side facing video camera field of view with the red event light on the left border focused on the region outside the front door and a lower boundary just below the bottom edge of the compartment (BSEE 243).

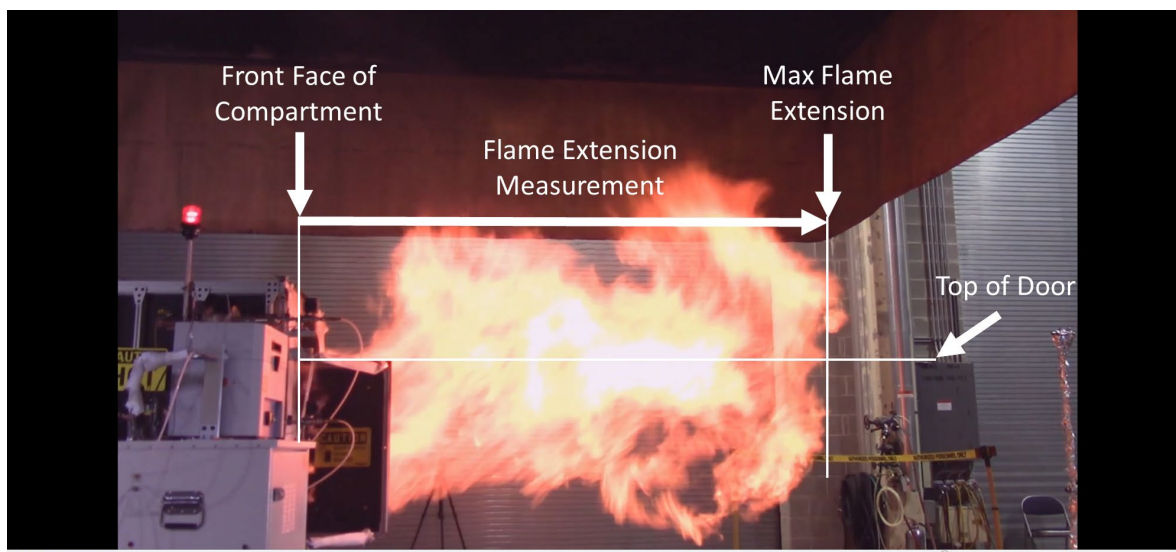


Fig. 28. Horizontal flame extension measurement at the top of the door from the front face of the compartment out to the furthest flame front extension for the left camera (BSEE 239).

3. Results and Discussion

3.1. Backdraft Events and Non-events

Pressure, heat flux, and temperature measurements for representative backdraft experiments are provided in Figs. 29-38, including photos of the fire size, a non-event, and a backdraft event. As previously stated, at the beginning of each experiment, the compartment burner was ignited while the front entryway remained open. As the flame reached a quasi-equilibrium state, the compartment temperatures and heat flux to the compartment floor were observed to increase, as indicated within the first 60 s of the heat flux gauge and thermocouple measurements. The compartment door was then closed 60 s after igniting the burner, at which time the differential pressure between the interior and exterior of the compartment spiked.

While the compartment door was closed, fuel was continuously fed to the burner, which sustained a flame within the compartment. As the flame continued to burn, the flame diminished, as observed by a decrease in the temperature and internal heat flux. Once the flame was extinguished, minor spikes in the temperature and heat flux were occasionally observed, attributed to local ignitions occurring within the compartment.

When the compartment door opened and a backdraft event occurred, heat flux and temperature measurements increased substantially. Differential pressure measurements were also found to initially decrease to negative pressure, caused by the rapid opening of the doorway, then peak when a backdraft event occurred. In a non-event case, temperature and heat flux values continued to decline when the flame was extinguished. Furthermore, no pressure peak was observed when a non-backdraft event occurred, yet pressure pulses and negative peaks were found when the doorway was closed and opened, respectively, and were also attributed to local ignitions within the compartment while the door was closed.

As shown from Figs. 29-38, the general procedure described was observed for all experiments, regardless of compartment configurations. The agreement of the repeated measurements before an anticipated backdraft event demonstrated the compartment's ability to maintain consistency across multiple runs. The compartment's ability to host repeatable experiments affirms its strong integrity, which is essential to establish a correlation between variable compartment configurations and backdraft events.

Clear distinctions between non-events and events wherein non-event pressure, heat flux, and temperature peaks were lower than measurements obtained when a backdraft event occurred. Before the door opening, the time-series data, pressure, heat flux, and temperature measurements were reasonably consistent for repeated conditions, regardless of a backdraft event. When the compartment door was opened, and a backdraft event occurred, the heat flux and temperature measurements were observed to increase substantially compared to a non-event. The transition from no ignition to increasingly more prominent backdrafts was observed for each fuel as its flow time was increased.

Comparing these experiment results to previous research studies is difficult due to the differences in compartment configurations (e.g., compartment size, fuel type, fire size, fuel time, spark ignition locations, spark delay time, front opening). A general comparison can be made, however, to Fleischmann's reduced-scale compartment results [11]. For the same methane fuel, in a similar-sized reduced-scale compartment, but with a larger fire size, he reported higher temperatures, higher pressures, and longer horizontal flame extension as would be expected.

Methane 25.0 kW

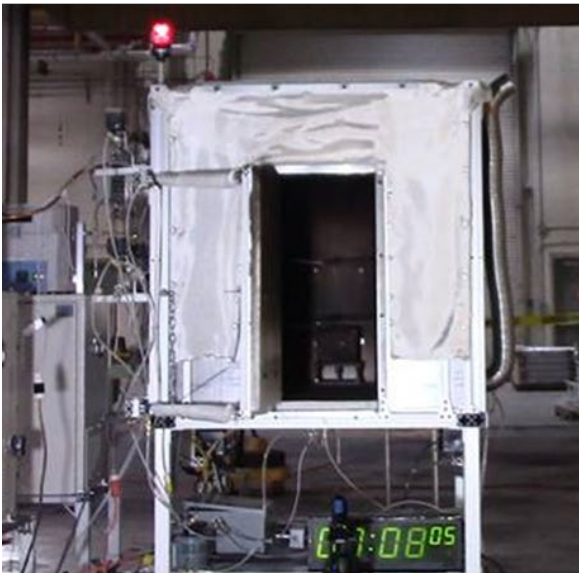


Fig. 29. A representative 25.0 kW methane fire after ignition (top, BSEE 61), a non-event after the front opens (bottom left, BSEE 61), and maximum flame extension during a backdraft event (bottom right, BSEE 52).

Methane 37.5 kW

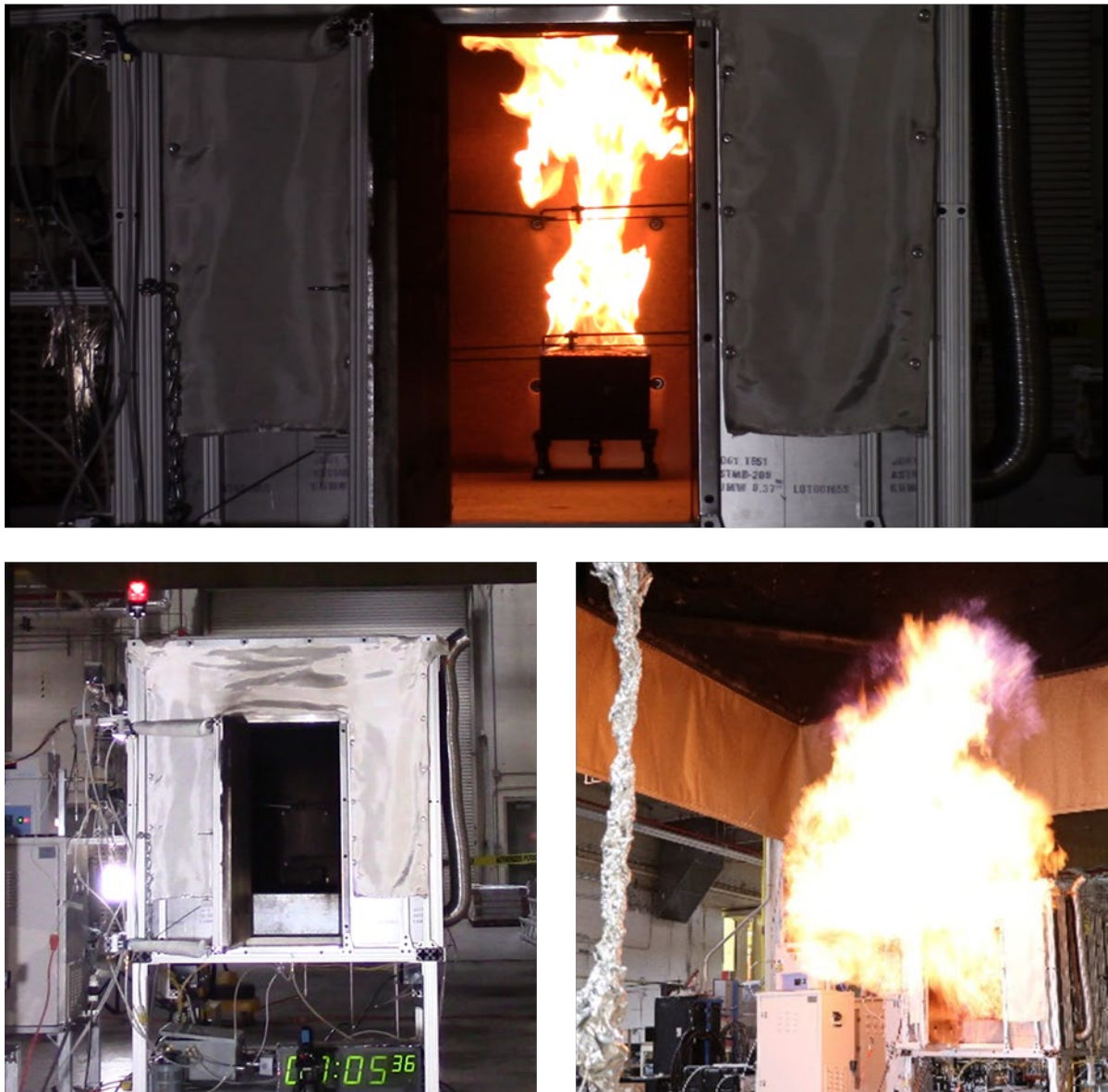


Fig. 30. A representative 37.5 kW methane fire after ignition (top, BSEE 103), a non-event after the front opens (bottom left, BSEE 109), and maximum flame extension during a backdraft event (bottom right, BSEE 103).

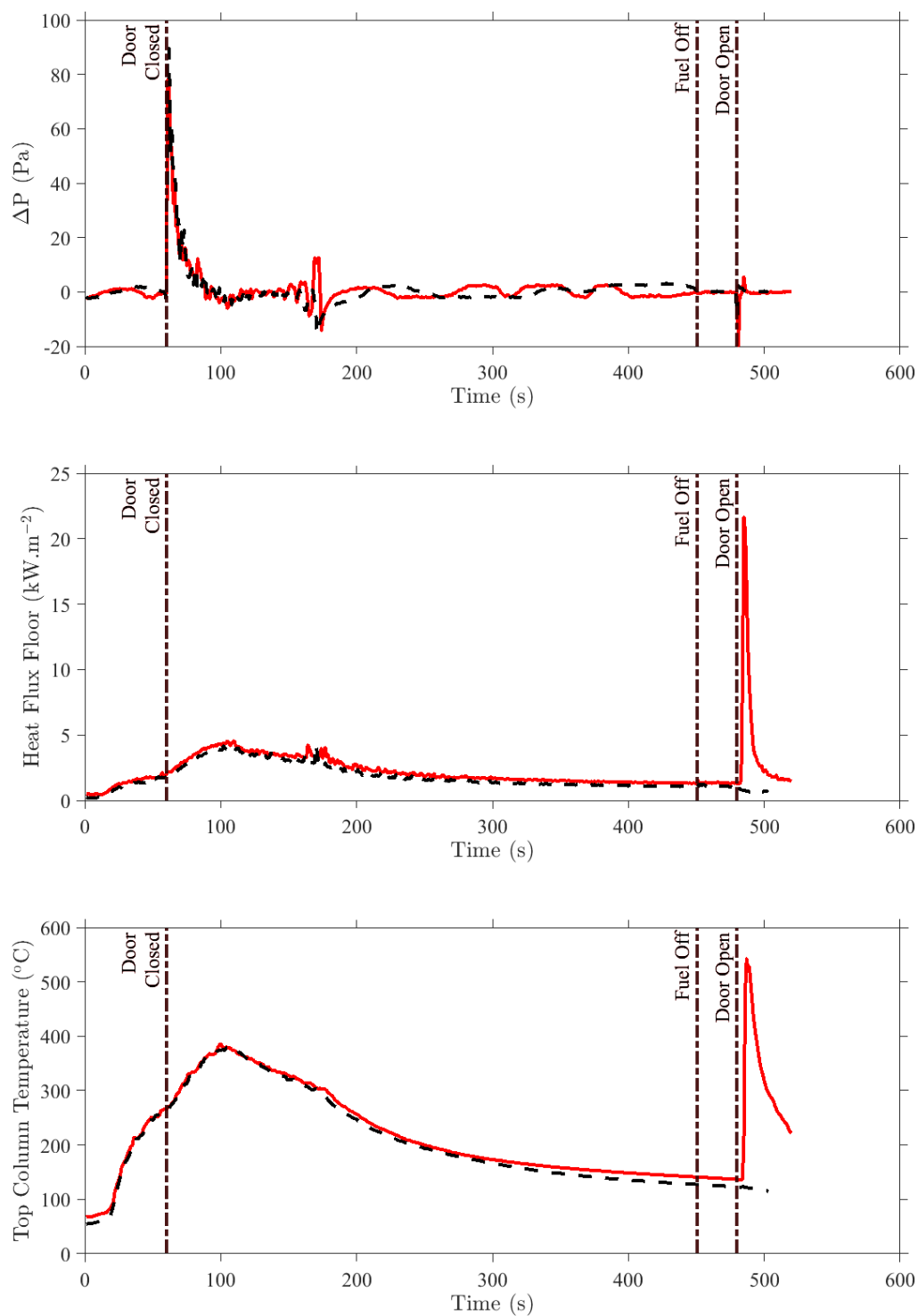


Fig. 31. Pressure, heat flux, temperature measurements for a 25.0 kW methane fire. Note the temperature spikes at 480 s (450 s fuel time plus 30 s until the door opens) when the front opens for the backdraft event (red line) compared to the non-event (black dashed line) (non-event BSEE 61, event BSEE 52). Expanded uncertainties in the measurements were estimated from Type B evaluation of uncertainties to be 0.15 % for pressure, 3.0 % for heat flux, and 2.20 $^{\circ}\text{C}$ or 0.75 % (whichever is greater) for temperature.

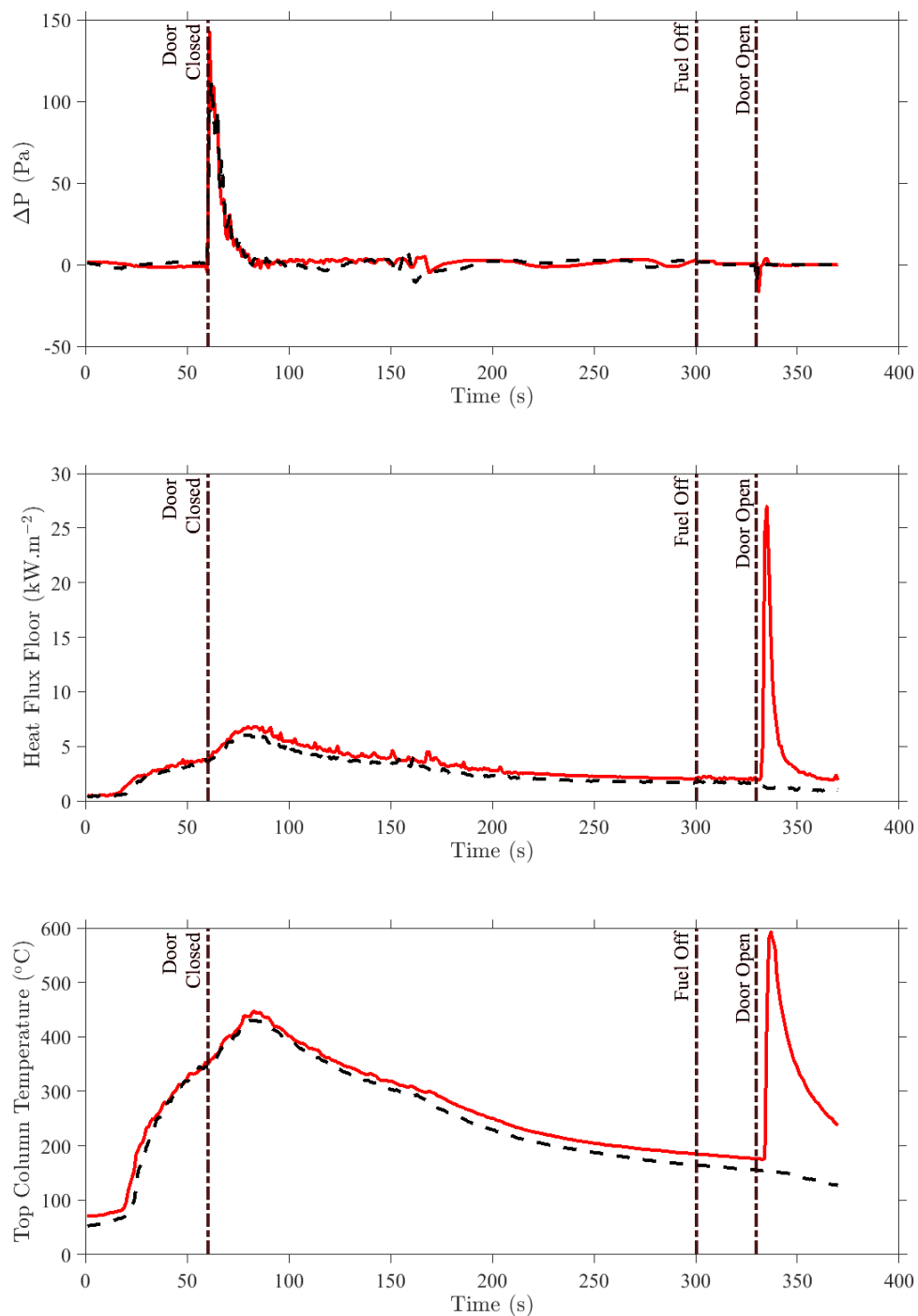


Fig. 32. Pressure, heat flux, temperature measurements for a 37.5 kW methane fire. Note the temperature spikes at 330 s (300 s of fuel plus 30 s) after the front opens for the backdraft event (red line) compared to the non-event (black dashed line) (non-event BSEE 109, event BSEE 103). Expanded uncertainties in the measurements were estimated from Type B evaluation of uncertainties to be 0.15 % for pressure, 3.0 % for heat flux, and 2.20 $^{\circ}\text{C}$ or 0.75 % (whichever is greater) for temperature.

Propane 16.7 kW



Fig. 33. A representative 16.7 kW propane fire after ignition (top, BSEE 203), a non-event after the front opens (bottom left, BSEE 203), and maximum flame extension during a backdraft event (bottom right, BSEE 191).

Propane 25.0 kW



Fig. 34. A representative 25.0 kW propane fire after ignition (top, BSEE 132), a non-event after the front opens (bottom left, BSEE 132), and maximum flame extension during a backdraft event (bottom right, BSEE 167).

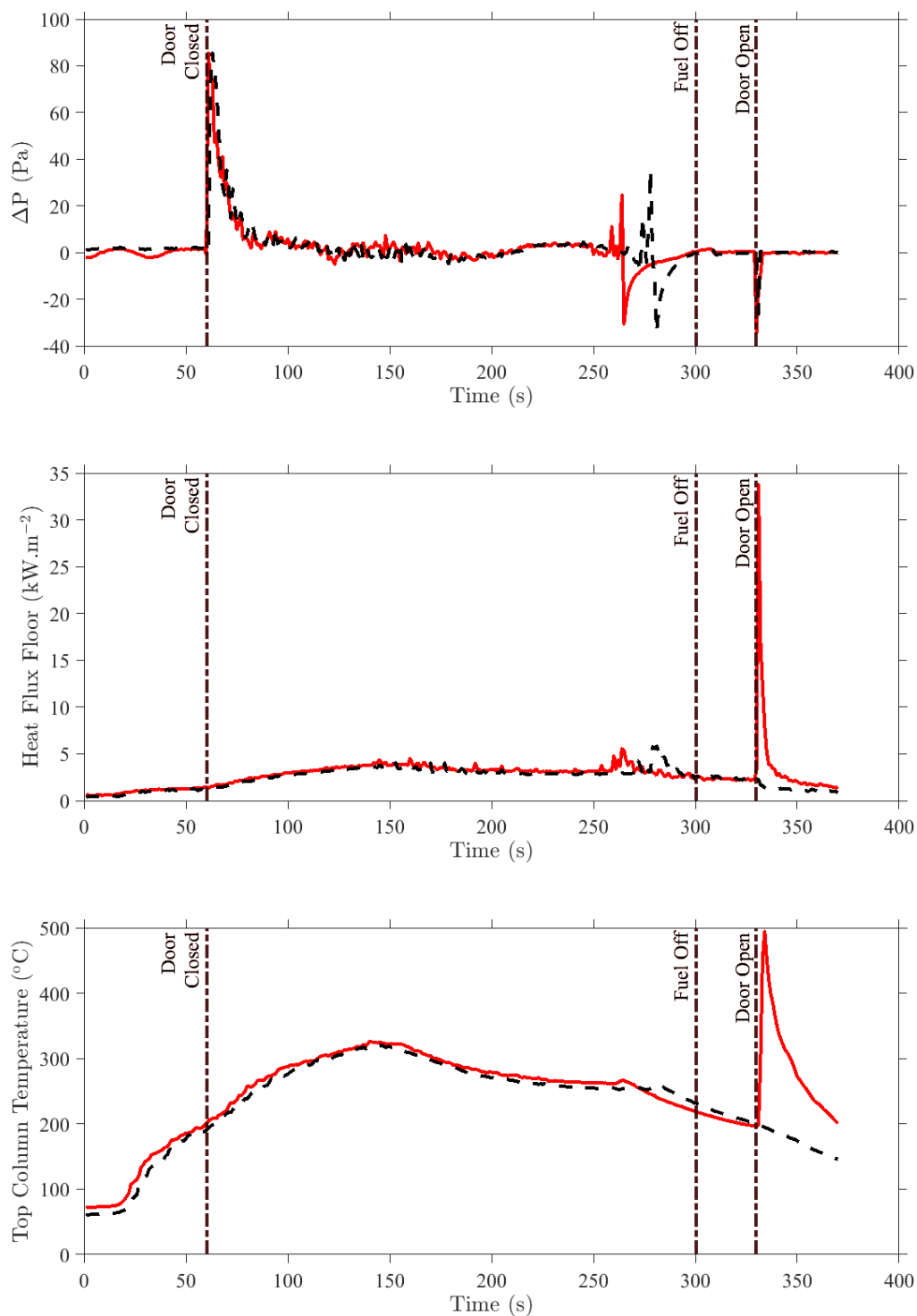


Fig. 35. Pressure, heat flux, temperature measurements for a 16.7 kW propane fire. Note the temperature spikes at 330 s (300 s of fuel plus 30 s) after the front opens for the backdraft event (red line) compared to the non-event (black dashed line) (non-event BSEE 213, event BSEE 197). Expanded uncertainties in the measurements were estimated from Type B evaluation of uncertainties to be 0.15 % for pressure, 3.0 % for heat flux, and 2.20 °C or 0.75 % (whichever is greater) for temperature.

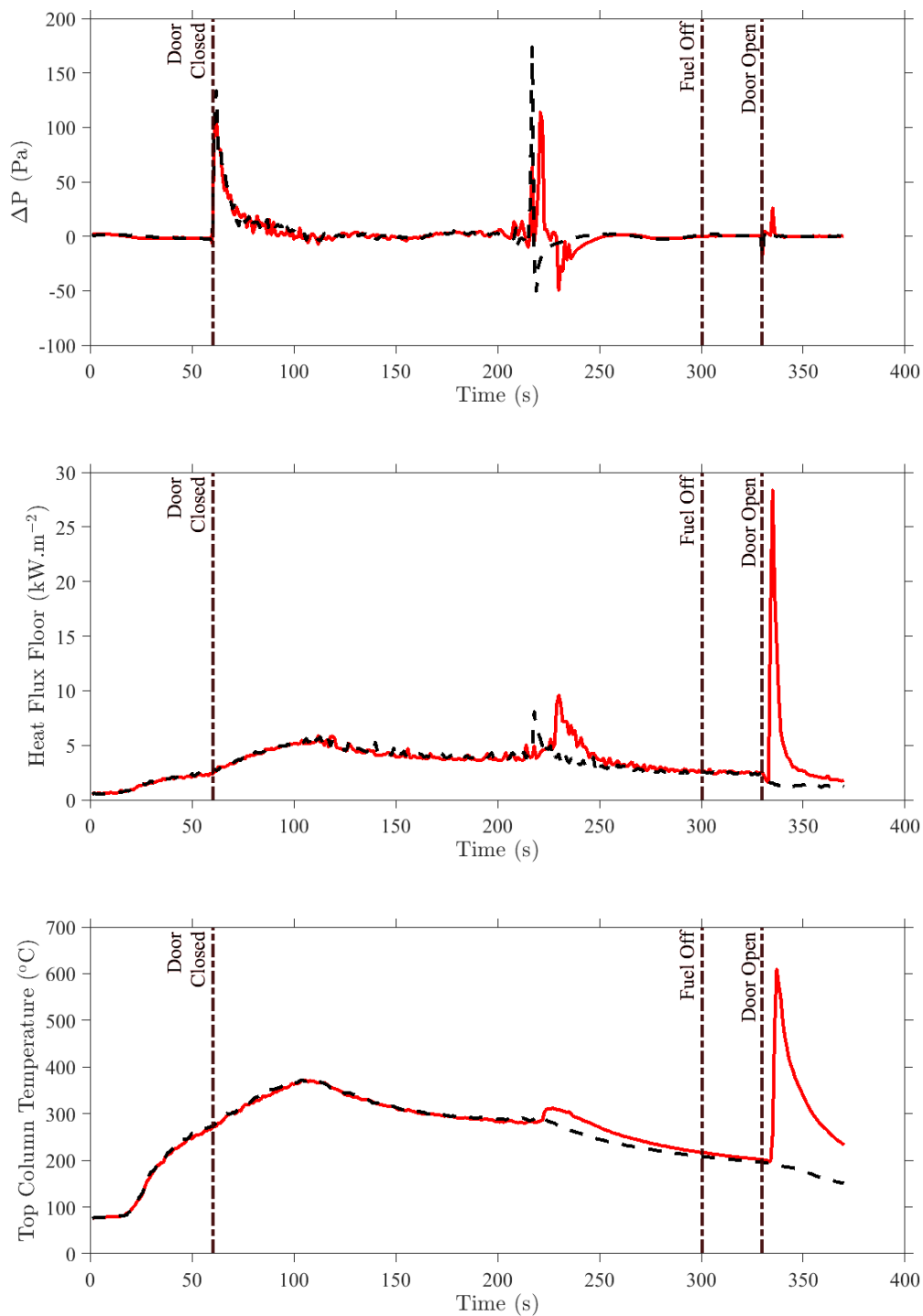


Fig. 36. Pressure, heat flux, temperature measurements for a 25.0 kW propane fire. Note the temperature spikes at 330 s (300 s of fuel plus 30 s) after the front opens for the backdraft event (red line) compared to the non-event (black dashed line) (non-event BSEE 153, event BSEE 150). Expanded uncertainties in the measurements were estimated from Type B evaluation of uncertainties to be 0.15 % for pressure, 3.0 % for heat flux, and 2.20 $^{\circ}\text{C}$ or 0.75 % (whichever is greater) for temperature.

Propene 25.0 kW

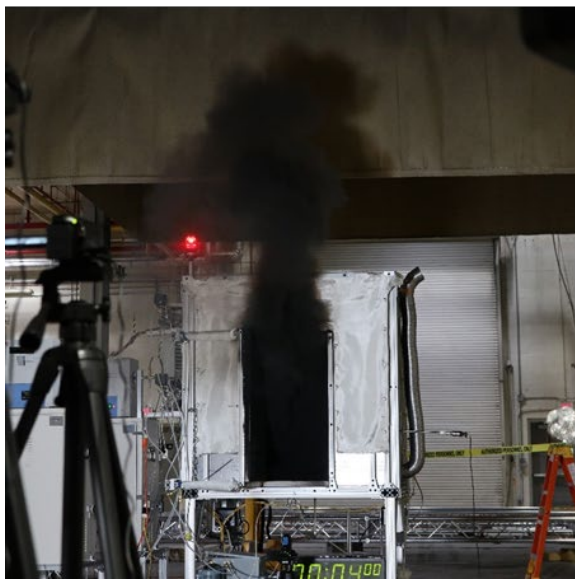
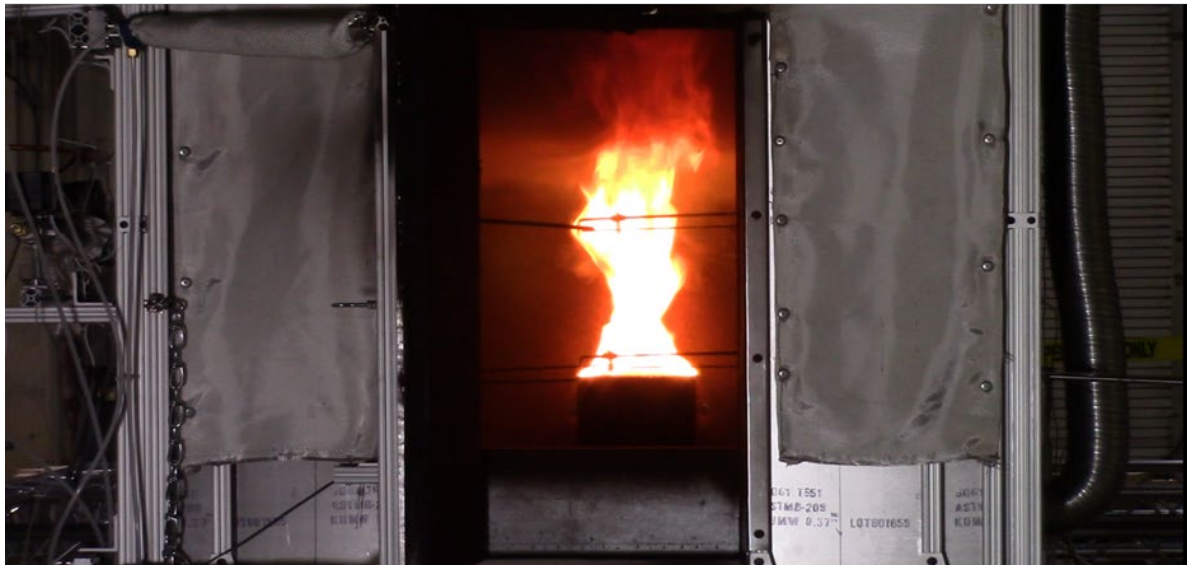


Fig. 37. A representative 25.0 kW propene fire after ignition (top, BSEE 222), a non-event after the front opens (bottom left, BSEE 222), and maximum flame extension during a backdraft event (bottom right, BSEE 226). Note the layering within the compartment in the top image where the top of the flame is within the dark upper layer. Also note the dark smoke from the compartment in the non-event image (bottom left). The flame extension is easily observed mixed with the smoke that pushed outward from within the compartment during a backdraft event (bottom right).

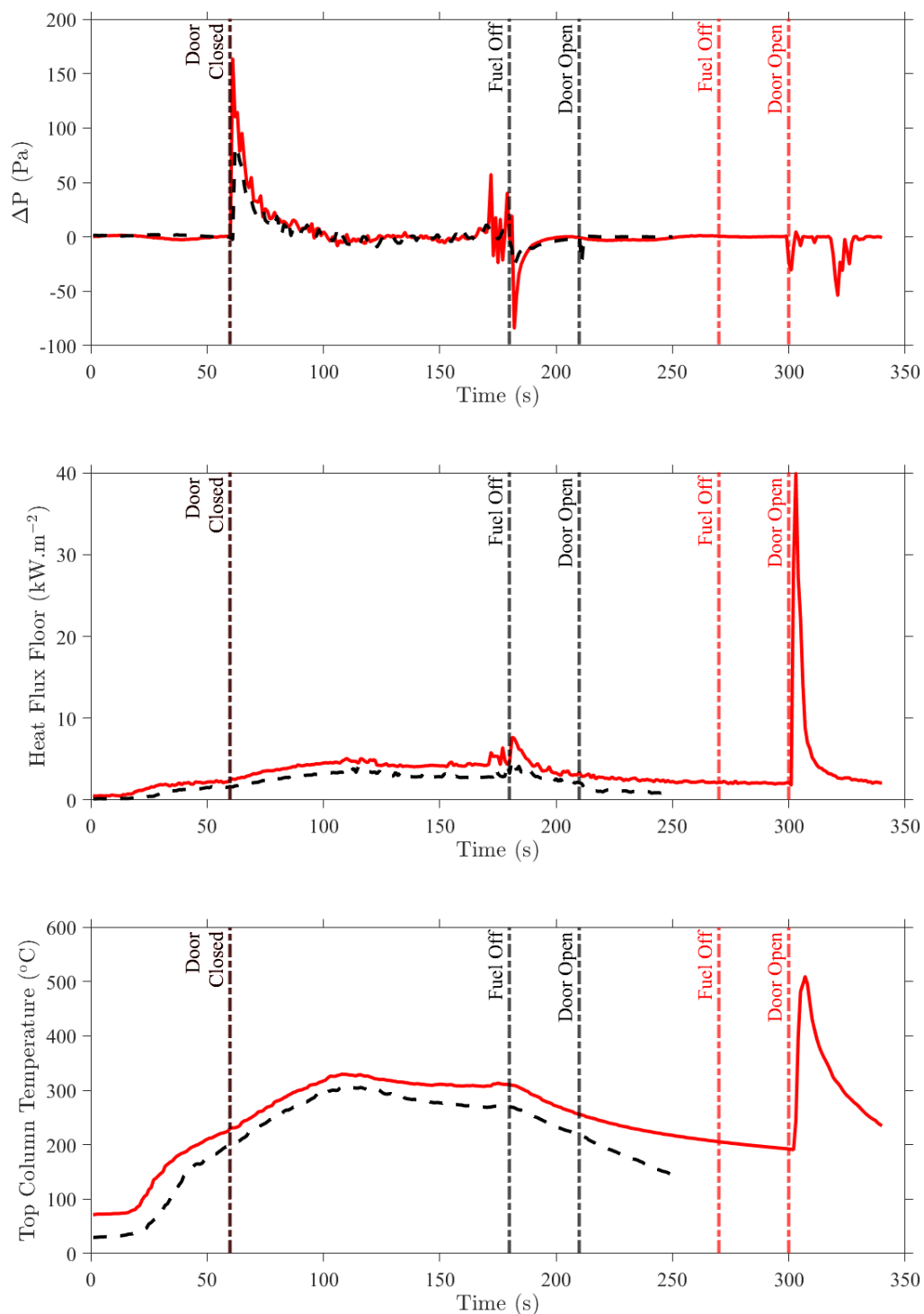


Fig. 38. Pressure, heat flux, temperature measurements for a 25.0 kW propene fire. Note the temperature spikes at 300 s (270 s of fuel plus 30 s) after the front opens for the backdraft event (red line) compared to the non-event (black dashed line) (non-event BSEE 221, event BSEE 237). Expanded uncertainties in the measurements were estimated from Type B evaluation of uncertainties to be 0.15 % for pressure, 3.0 % for heat flux, and 2.20 $^{\circ}\text{C}$ or 0.75 % (whichever is greater) for temperature.

3.2. Measurements from Experiments

Pressure, temperature, and heat flux measurements in addition to ignition delay time relative to the door opening, horizontal flame extension, and maximum vertical flame depth relative to the door vertical opening are reported in Tables 2-19. The maximum pressure and heat flux values were the peak readings after the compartment door opened. Temperature measurements were averaged during the 10 s before the front door opened. Uncertainties in the measurements were estimated from Type B evaluation of uncertainties detailed previously in Section 2. There are clear distinctions between non-events and events wherein non-event pressure, heat flux, and spatial measurements were lower than measurements obtained when a backdraft event occurred.

Spark delay in the following tables is noted as either a 0 s or 5 s delay from the door opening to initiation of a spark. There were a few cases very early in the experiments where a 2 s spark delay was used. The results between these few cases and the 0 s spark delay were similar, and therefore the 2 s spark delay experiments were listed as a 0 s spark delay. The 5 s spark delay experiments are noted separately in the following tables (“#,5”).

If ignition was reported (a ‘Yes’ is noted in the Ignition column) but the combustion remained within the compartment with no flame extension outside the compartment, horizontal flame extension, and the maximum vertical flame depth relative to the front door were not measured and are represented by a dash in the tables.

The external heat flux gauge was not used before BSEE 41; therefore, a dash was used in the tables. The ignition delay time, noted under “Ign. Time” in the tables, is defined as the difference between when the front door begins to open and when ignition is observed within the compartment. The maximum vertical depth of flame extension measured down from the top of the compartment door and reported as a percentage of the front door opening, regardless of the door or window configuration, is listed under the table column heading “Vert Flame Depth.”

Methane – 25.0 kW Fire Size – Door Configuration – Low Spark Position

The measurements summarized from the 25.0 kW methane fire with the door configuration and low spark position are shown in Table 2. Fuel-off times for the 25.0 kW fire size range from 390 s to 450 s, a higher range than for the 37.5 kW methane fires with the same conditions.

Table 2. Measurements for the 25.0 kW methane experiments with a door configuration and a low spark position.

Fuel-off Time (s)	Ign.	P_{\max} (Pa)	Max Heat Flux Flr. (kW/m ²)	Max Heat Flux Ext. (kW/m ²)	T_{avg} High (°C)	T_{avg} Low (°C)	Ign. Time (s)	Horiz Flame Ext. (m)	Vert Flame Depth (%)	Exp
390	No	4.2	1.5	-	144.6	126.2	-	-	-	BSEE 018
390	No	5.4	0.6	-	111.9	90.7	-	-	-	BSEE 021
420	No	5.2	0.8	-	118.6	101.4	-	-	-	BSEE 022
420	No	5.8	0.8	-	109.0	91.3	-	-	-	BSEE 030
420	Yes	8.3	20.5	-	138.8	123.1	1.2	1.1	91.5	BSEE 039
420	Yes	6.4	24.2	3.0	147.7	133.6	0.8	1.5	137.1	BSEE 128
450	Yes	3.2	13.8	-	136.6	121.9	3.5	-	-	BSEE 020
450	Yes	6.4	19.9	-	121.2	106.6	3.1	1.5	103.0	BSEE 023
450	No	6.0	1.4	0.0	114.4	99.2	-	-	-	BSEE 041
450	Yes	8.0	14.8	1.6	121.3	106.3	1.7	0.9	77.3	BSEE 042
450	Yes	3.3	21.1	2.5	110.3	95.3	1.8	1.3	103.0	BSEE 060
450,5	No	1.4	1.7	0.0	124.1	108.9	-	-	-	BSEE 061
450,5	No	1.0	1.8	0.0	138.5	123.2	-	-	-	BSEE 072

Ign.=ignition, P_{\max} =maximum pressure, Flr.=floor, Ext.= External location for the heat flux gauge, T_{avg} =average temperature, Horiz=horizontal, Vert=vertical, Exp=experiment ID.

Methane – 25.0 kW Fire Size – Door Configuration – Middle Spark Position

The measurements summarized from the 25.0 kW methane fire with the door configuration and middle spark position are shown in Table 3. Fuel-off times for the 25.0 kW fire size range from 360 s to 450 s, a higher range than for the 37.5 kW methane fires with the same conditions.

Table 3. Measurements for the 25.0 kW methane experiments with a door configuration and a middle spark position.

Fuel-off Time (s)	Ign.	P_{\max} (Pa)	Max Heat Flux Flr. (kW/m ²)	Max Heat Flux Ext. (kW/m ²)	T_{avg} High (°C)	T_{avg} Low (°C)	Ign. Time (s)	Horiz Flame Ext. (m)	Vert Flame Depth (%)	Exp
360	No	6.8	2.0	0.1	145.4	124.8	-	-	-	BSEE 043
390	No	5.9	2.1	0.1	138.8	120.8	-	-	-	BSEE 044
390	Yes	1.2	10.2	0.5	135.1	118.0	2.7	0.6	23.0	BSEE 084
390	Yes	4.8	15.4	1.9	153.2	138.0	2.4	1.4	119.8	BSEE 127
420	Yes	6.4	12.2	1.0	142.1	125.8	2.4	0.7	88.4	BSEE 045
420	Yes	2.0	11.7	0.8	148.0	131.7	2.5	0.6	42.9	BSEE 046
450	Yes	3.3	15.6	1.5	132.3	117.5	2.6	1.1	94.2	BSEE 047
450	Yes	3.2	20.0	2.1	134.0	119.5	2.5	1.5	117.2	BSEE 073
450,5	Yes	2.0	15.5	0.7	131.6	115.8	5.6	0.8	42.9	BSEE 057
450,5	Yes	1.6	14.6	0.8	142.3	127.3	5.1	0.8	28.7	BSEE 074

Ign.=ignition, P_{\max} =maximum pressure, Flr.=floor, Ext.= External location for the heat flux gauge, T_{avg} =average temperature, Horiz=horizontal, Vert=vertical, Exp=experiment ID.

Methane – 25.0 kW Fire Size – Window Configuration – Low Spark Position

The measurements summarized from the 25.0 kW methane fire with the window configuration and low spark position are shown in Table 4. Fuel-off times for the 25.0 kW fire size range from 360 s to 450 s, a higher range than for the 37.5 kW methane fires with similar conditions.

Table 4. Measurements made for the 25.0 kW methane experiments with a window configuration and a low spark position.

Fuel-off Time (s)	Ign.	P_{\max} (Pa)	Max Heat Flux Flr. (kW/m ²)	Max Heat Flux Ext. (kW/m ²)	T_{avg} High (°C)	T_{avg} Low (°C)	Ign. Time (s)	Horiz Flame Ext. (m)	Vert Flame Depth (%)	Exp
360	No	8.2	1.0	-	125.9	101.7	-	-	-	BSEE 032
360	Yes	1.1	1.6	0.0	144.3	121.9	3.0	-	-	BSEE 068
390	Yes	5.5	14.6	-	122.8	103.6	2.0	0.6	48.6	BSEE 033
390	Yes	8.8	1.0	-	117.3	96.7	3.6	-	-	BSEE 035
390	Yes	2.8	9.4	0.1	130.0	109.8	4.0	0.5	28.7	BSEE 062
420	Yes	7.2	14.0	-	125.5	108.2	2.1	0.8	68.5	BSEE 034
420	Yes	6.7	17.3	-	125.5	108.1	3.2	1.7	77.3	BSEE 036
450	Yes	5.3	21.2	3.2	129.7	113.5	1.8	1.9	137.1	BSEE 063
450	Yes	6.4	21.5	3.1	117.7	102.3	1.4	1.9	125.6	BSEE 067
450	Yes	7.1	24.5	3.7	123.2	107.3	1.7	2.4	128.6	BSEE 069
450,5	No	0.9	1.4	0.1	134.0	117.5	-	-	-	BSEE 064
450,5	Yes	3.8	17.4	1.2	124.9	109.2	5.0	1.1	74.3	BSEE 071
450,5	No	1.2	1.0	0.2	113.0	98.3	-	-	-	BSEE 105

Ign.=ignition, P_{\max} =maximum pressure, Flr.=floor, Ext.= External location for the heat flux gauge, T_{avg} =average temperature, Horiz=horizontal, Vert=vertical, Exp=experiment ID.

Methane – 25.0 kW Fire Size – Window Configuration – Middle Spark Position

The measurements summarized from the 25.0 kW methane fire with the window configuration and middle spark position are shown in Table 5. Fuel-off times for the 25.0 kW fire size range from 360 s to 450 s, a higher range than for the 37.5 kW methane fires with similar conditions.

Table 5. Measurements for the 25.0 kW methane experiments with a window configuration and a middle spark position.

Fuel-off Time (s)	Ign.	P_{\max} (Pa)	Max Heat Flux Flr. (kW/m ²)	Max Heat Flux Ext. (kW/m ²)	T_{avg} High (°C)	T_{avg} Low (°C)	Ign. Time (s)	Horiz Flame Ext. (m)	Vert Flame Depth (%)	Exp
360	Yes	1.9	10.1	0.2	148.7	125.1	1.9	0.5	11.5	BSEE 056
360	Yes	1.8	1.8	0.1	145.9	124.0	*	-	-	BSEE 058
360	Yes	4.5	12.0	0.9	147.4	131.9	2.7	1.0	51.3	BSEE 220
390	Yes	1.5	11.4	0.5	149.0	130.6	2.3	0.5	31.4	BSEE 051
420	Yes	7.0	15.7	1.6	121.7	103.8	2.5	1.6	91.5	BSEE 049
420	Yes	5.4	17.5	2.1	123.6	103.6	2.2	1.2	119.8	BSEE 054
450	Yes	15.7	23.5	3.5	128.3	112.6	2.4	2.3	137.1	BSEE 050
450	Yes	8.0	23.1	3.2	137.6	122.0	2.6	2.3	137.1	BSEE 052
450,5	Yes	3.7	18.5	1.4	129.4	111.8	4.9	1.0	77.3	BSEE 055
450,5	Yes	5.6	16.6	1.3	130.3	114.1	6.3	1.0	77.0	BSEE 065

Ign.=ignition, P_{\max} =maximum pressure, Flr.=floor, Ext.= External location for the heat flux gauge, T_{avg} =average temperature, Horiz=horizontal, Vert=vertical, Exp=experiment ID.

* ignition delay time was not measured because the ignition was not observed in the video.

Methane – 37.5 kW Fire Size – Door Configuration – Low Spark Position

The measurements summarized from the 37.5 kW methane fire with the door configuration and low spark position are shown in Table 6. Fuel-off times for the 37.5 kW fire size range from 240 s to 300 s, a lower range than for the 25.0 kW methane fires with similar conditions.

Table 6. Measurements for the 37.5 kW methane experiments with a door configuration and a low spark position.

Fuel-off Time (s)	Ign.	P_{\max} (Pa)	Max Heat Flux Flr. (kW/m ²)	Max Heat Flux Ext. (kW/m ²)	T_{avg} High (°C)	T_{avg} Low (°C)	Ign. Time (s)	Horiz Flame Ext. (m)	Vert Flame Depth (%)	Exp
240	Yes	0.9	2.4	0.2	178.3	144.1	*	-	-	BSEE 087
240	Yes	0.6	2.4	0.1	180.9	151.1	*	-	-	BSEE 130
270	Yes	6.2	14.0	1.7	172.0	148.6	3.0	1.5	65.9	BSEE 096
270	Yes	1.0	2.8	0.1	186.7	167.5	*	-	-	BSEE 116
300	Yes	4.5	32.3	2.7	173.2	154.3	0.7	1.5	88.4	BSEE 090
300	Yes	10.1	26.8	0.6	175.7	159.7	0.3	0.7	34.5	BSEE 117
300	Yes	8.0	26.3	3.0	178.4	160.0	0.5	1.7	108.7	BSEE 125
300,5	No	0.8	2.9	0.2	177.5	158.7	-	-	-	BSEE 091
300,5	No	1.3	3.0	0.1	184.1	167.9	-	-	-	BSEE 118

Ign.=ignition, P_{\max} =maximum pressure, Flr.=floor, Ext.= External location for the heat flux gauge, T_{avg} =average temperature, Horiz=horizontal, Vert=vertical, Exp=experiment ID.
* ignition delay time was not measured because the ignition was not observed in the video.

Methane – 37.5 kW Fire Size – Door Configuration – Middle Spark Position

The measurements summarized from the 37.5 kW methane fire with the door configuration and middle spark position are shown in Table 7. Fuel-off times for the 37.5 kW fire size range from 240 s to 300 s, a lower range than for the 25.0 kW methane fires with similar conditions.

Table 7. Measurements for the 37.5 kW methane experiments with a door configuration and a middle spark position.

Fuel-off Time (s)	Ign.	P_{\max} (Pa)	Max Heat Flux Flr. (kW/m ²)	Max Heat Flux Ext. (kW/m ²)	T_{avg} High (°C)	T_{avg} Low (°C)	Ign. Time (s)	Horiz Flame Ext. (m)	Vert Flame Depth (%)	Exp
240	Yes	2.4	12.9	0.8	202.1	171.4	2.0	0.7	48.6	BSEE 098
240	Yes	2.1	13.3	0.9	207.0	178.0	1.8	0.8	37.1	BSEE 114
270	Yes	2.3	13.2	1.3	188.2	167.6	2.0	0.8	45.6	BSEE 099
270	Yes	6.1	17.0	1.8	188.9	168.8	2.2	1.5	77.0	BSEE 126
300	Yes	3.2	25.7	3.1	177.7	160.8	2.3	1.4	119.8	BSEE 101
300	Yes	5.7	24.1	2.8	178.9	162.3	2.3	1.5	125.6	BSEE 113
300,5	Yes	1.4	15.6	0.9	179.8	162.3	5.3	0.8	48.6	BSEE 100
300,5	Yes	2.7	15.6	0.9	180.8	163.9	5.2	0.8	65.9	BSEE 115

Ign.=ignition, P_{\max} =maximum pressure, Flr.=floor, Ext.= External location for the heat flux gauge, T_{avg} =average temperature, Horiz=horizontal, Vert=vertical, Exp=experiment ID.

Methane – 37.5 kW Fire Size – Window Configuration – Low Spark Position

The measurements summarized from the 37.5 kW methane fire with the window configuration and low spark position are shown in Table 8. Fuel-off times for the 37.5 kW fire size range from 240 s to 300 s, a lower range than for the 25.0 kW methane fires with similar conditions.

Table 8. Measurements for the 37.5 kW methane experiments with a window configuration and a low spark position.

Fuel-off Time (s)	Ign.	P_{\max} (Pa)	Max Heat Flux Flr. (kW/m ²)	Max Heat Flux Ext. (kW/m ²)	T_{avg} High (°C)	T_{avg} Low (°C)	Ign. Time (s)	Horiz Flame Ext. (m)	Vert Flame Depth (%)	Exp
240	No	0.7	2.7	0.2	194.2	161.7	-	-	-	BSEE 092
240	Yes	1.6	9.6	0.2	191.4	165.4	3.2	0.4	28.7	BSEE 112
270	Yes	6.1	24.9	2.6	183.6	160.4	1.5	1.9	91.5	BSEE 093
270	Yes	2.8	16.3	0.4	170.1	142.7	2.2	0.5	25.7	BSEE 106
300	Yes	6.5	34.8	3.0	176.0	156.4	1.6	2.1	117.2	BSEE 094
300	Yes	5.7	25.2	3.3	171.6	151.5	1.6	2.0	71.6	BSEE 107
300,5	Yes	3.0	16.7	1.1	168.6	148.4	5.3	1.1	57.0	BSEE 097
300,5	No	1.1	1.9	0.2	157.3	138.1	-	-	-	BSEE 109

Ign.=ignition, P_{\max} =maximum pressure, Flr.=floor, Ext.= External location for the heat flux gauge, T_{avg} =average temperature, Horiz=horizontal, Vert=vertical, Exp=experiment ID.

Methane – 37.5 kW Fire Size – Window Configuration – Middle Spark Position

The measurements summarized from the 37.5 kW methane fire with the window configuration and middle spark position are shown in Table 9. Fuel-off times for the 37.5 kW fire size range from 240 s to 300 s, a lower range than for the 25.0 kW methane fires with similar conditions.

Table 9. Measurements for the 37.5 kW methane experiments with a window configuration and a middle spark position.

Fuel-off Time (s)	Ign.	P _{max} (Pa)	Max Heat Flux Flr. (kW/m ²)	Max Heat Flux Ext. (kW/m ²)	T _{avg} High (°C)	T _{avg} Low (°C)	Ign. Time (s)	Horiz Flame Ext. (m)	Vert Flame Depth (%)	Exp
240	Yes	1.4	13.2	0.4	202.8	172.1	2.6	0.6	37.1	BSEE 102
240	Yes	49.5	8.8	0.3	193.5	161.1	2.2	0.4	23.0	BSEE 124
270	Yes	3.6	15.6	1.3	177.2	155.1	2.3	0.7	57.0	BSEE 110
270	Yes	4.2	10.2	0.5	165.1	138.2	2.6	0.5	37.1	BSEE 123
270	Yes	3.1	11.8	0.6	171.8	153.2	2.3	0.6	28.7	BSEE 216
300	Yes	10.7	30.1	3.8	177.7	159.0	2.1	1.9	117.2	BSEE 103
300	Yes	9.1	27.4	3.5	172.4	154.7	2.0	2.1	119.8	BSEE 119
300	Yes	4.6	13.1	2.0	130.2	108.0	2.7	1.1	103.0	BSEE 135
300,5	Yes	2.8	16.7	1.2	176.5	158.4	4.8	1.0	39.8	BSEE 111
300,5	Yes	6.7	18.1	1.4	179.8	162.4	4.8	1.2	77.0	BSEE 120

Ign.=ignition, P_{max}=maximum pressure, Flr.=floor, Ext.= External location for the heat flux gauge, T_{avg}=average temperature, Horiz=horizontal, Vert=vertical, Exp=experiment ID.

Propane – 16.7 kW Fire Size – Door Configuration – Low Spark Position

The measurements summarized from the 16.7 kW propane fire with the door configuration and low spark position are shown in Table 10. Fuel-off times for the 16.7 kW fire size range from 270 s to 330 s, a higher range than for the 25.0 kW propane fires with similar conditions.

Table 10. Measurements for the 16.7 kW propane experiments with a door configuration and a low spark position.

Fuel-off Time (s)	Ign.	P_{\max} (Pa)	Max Heat Flux Flr. (kW/m ²)	Max Heat Flux Ext. (kW/m ²)	T_{avg} High (°C)	T_{avg} Low (°C)	Ign. Time (s)	Horiz Flame Ext. (m)	Vert Flame Depth (%)	Exp
270	No	1.9	3.4	0.1	235.0	182.9	-	-	-	BSEE 179
270	No	2.5	3.5	0.1	227.4	174.4	-	-	-	BSEE 214
300	Yes	8.4	25.2	0.2	200.3	170.1	0.6	1.5	122.9	BSEE 176
300	Yes	8.9	20.4	0.1	190.3	161.1	0.7	1.5	108.7	BSEE 208
330	Yes	9.1	42.5	0.6	188.0	165.4	0.5	1.9	131.3	BSEE 178
330	Yes	12.9	42.6	0.3	179.0	155.9	0.5	2.1	131.3	BSEE 206
330, 5	No	1.6	1.7	0.1	188.6	165.2	-	-	-	BSEE 180
330, 5	No	1.5	1.3	0.1	176.2	152.1	-	-	-	BSEE 207

Ign.=ignition, P_{\max} =maximum pressure, Flr.=floor, Ext.= External location for the heat flux gauge, T_{avg} =average temperature, Horiz=horizontal, Vert=vertical, Exp=experiment ID.

Propane – 16.7 kW Fire Size – Door Configuration – Middle Spark Position

The measurements summarized from the 16.7 kW propane fire with the door configuration and middle spark position are shown in Table 11. Fuel-off times for the 16.7 kW fire size range from 270 s to 330 s, a higher range than for the 25.0 kW propane fires with similar conditions.

Table 11. Measurements for the 16.7 kW propane experiments with a door configuration and a middle spark position.

Fuel-off Time (s)	Ign.	P_{\max} (Pa)	Max Heat Flux Flr. (kW/m ²)	Max Heat Flux Ext. (kW/m ²)	T_{avg} High (°C)	T_{avg} Low (°C)	Ign. Time (s)	Horiz Flame Ext. (m)	Vert Flame Depth (%)	Exp
270	No	3.0	3.5	0.1	222.5	174.1	-	-	-	BSEE 192
270	No	1.6	3.0	0.1	228.1	169.5	-	-	-	BSEE 212
300	Yes	6.9	13.2	0.1	178.3	139.7	2.6	1.1	74.3	BSEE 190
300	No	1.2	2.7	0.1	205.4	164.5	-	-	-	BSEE 213
330	Yes	28.6	31.0	0.7	170.1	144.6	1.9	2.0	165.8	BSEE 191
330	Yes	14.6	20.2	0.2	182.2	149.4	2.3	1.7	131.3	BSEE 210
330,5	Yes	13.1	20.7	0.7	181.3	157.3	4.8	1.5	131.3	BSEE 193
330,5	Yes	7.4	14.1	0.4	175.8	148.1	6.1	1.2	85.8	BSEE 211

Ign.=ignition, P_{\max} =maximum pressure, Flr.=floor, Ext.= External location for the heat flux gauge, T_{avg} =average temperature, Horiz=horizontal, Vert=vertical, Exp=experiment ID.

Propane – 16.7 kW Fire Size – Window Configuration – Low Spark Position

The measurements summarized from the 16.7 kW propane fire with the window configuration and low spark position are shown in Table 12. Fuel-off times for the 16.7 kW fire size range from 270 s to 330 s, a higher range than for the 25.0 kW propane fires with similar conditions.

Table 12. Measurements for the 16.7 kW propane experiments with a window configuration and a low spark position.

Fuel-off Time (s)	Ign.	P_{\max} (Pa)	Max Heat Flux Flr. (kW/m ²)	Max Heat Flux Ext. (kW/m ²)	T_{avg} High (°C)	T_{avg} Low (°C)	Ign. Time (s)	Horiz Flame Ext. (m)	Vert Flame Depth (%)	Exp
270	No	1.4	2.9	0.1	227.1	173.2	-	-	-	BSEE 184
270	No	2.4	2.7	0.0	215.7	170.7	-	-	-	BSEE 205
300	Yes	5.9	10.7	0.2	204.0	167.0	1.2	1.0	68.5	BSEE 181
300	Yes	17.6	52.2	0.2	199.8	166.3	0.5	1.8	105.7	BSEE 197
330	Yes	22.2	60.1	0.4	176.6	147.4	0.4	2.0	128.6	BSEE 183
330	Yes	9.3	56.9	0.2	186.3	159.7	0.5	1.4	103.0	BSEE 199
330,5	No	1.7	2.6	0.2	193.6	165.8	-	-	-	BSEE 185
330,5	No	1.9	2.6	0.1	183.6	158.0	-	-	-	BSEE 198

Ign.=ignition, P_{\max} =maximum pressure, Flr.=floor, Ext.= External location for the heat flux gauge, T_{avg} =average temperature, Horiz=horizontal, Vert=vertical, Exp=experiment ID.

Propane – 16.7 kW Fire Size – Window Configuration – Middle Spark Position

The measurements summarized from the 16.7 kW propane fire with the window configuration and middle spark position are shown in Table 13. Fuel-off times for the 16.7 kW fire size range from 270 s to 330 s, a higher range than for the 25.0 kW propane fires with similar conditions.

Table 13. Measurements for the 16.7 kW propane experiments with a window configuration and a middle spark position.

Fuel-off Time (s)	Ign.	P_{\max} (Pa)	Max Heat Flux Flr. (kW/m ²)	Max Heat Flux Ext. (kW/m ²)	T_{avg} High (°C)	T_{avg} Low (°C)	Ign. Time (s)	Horiz Flame Ext. (m)	Vert Flame Depth (%)	Exp
270	No	1.5	3.4	0.1	238.9	185.1	-	-	-	BSEE 187
270	No	1.6	2.6	0.0	220.1	169.1	-	-	-	BSEE 203
300	Yes	5.0	11.7	0.2	208.5	174.8	2.3	1.1	85.8	BSEE 188
300	Yes	4.9	10.4	0.1	185.5	146.3	2.5	0.7	65.9	BSEE 201
330	Yes	19.8	24.2	0.4	199.3	171.0	1.8	2.0	137.1	BSEE 186
330	Yes	33.9	32.0	0.6	176.7	149.5	1.8	2.6	131.3	BSEE 202
330,5	Yes	11.0	16.1	0.3	181.3	150.8	5.0	1.8	85.8	BSEE 194
330,5	Yes	57.8	27.3	1.0	180.7	155.7	4.6	2.5	131.3	BSEE 204

Ign.=ignition, P_{\max} =maximum pressure, Flr.=floor, Ext.= External location for the heat flux gauge, T_{avg} =average temperature, Horiz=horizontal, Vert=vertical, Exp=experiment ID.

Propane – 25.0 kW Fire Size – Door Configuration – Low Spark Position

The measurements summarized from the 25.0 kW propane fire with the door configuration and low spark position are shown in Table 14. Fuel-off times for the 25.0 kW fire size range from 210 s to 300 s, a lower range than for the 16.7 kW propane fires with similar conditions.

Table 14. Measurements for the 25.0 kW propane experiments with a door configuration and a low spark position.

Fuel-off Time (s)	Ign.	P_{\max} (Pa)	Max Heat Flux Flr. (kW/m ²)	Max Heat Flux Ext. (kW/m ²)	T_{avg} High (°C)	T_{avg} Low (°C)	Ign. Time (s)	Horiz Flame Ext. (m)	Vert Flame Depth (%)	Exp
210	No	2.1	4.1	0.1	252.8	179.0	-	-	-	BSEE 131
240	No	0.8	4.2	0.2	258.3	207.9	-	-	-	BSEE 132
240	Yes	24.5	30.3	1.1	215.1	177.1	0.9	2.1	140.1	BSEE 161
240	Yes	1.8	3.8	0.0	238.2	198.4	*	-	-	BSEE 175
270	Yes	9.2	43.3	1.4	228.8	202.0	1.6	2.2	140.1	BSEE 133
270	Yes	16.1	32.3	1.1	216.6	190.5	1.7	2.2	134.4	BSEE 162
270	Yes	24.1	44.1	1.5	213.8	187.4	2.1	2.2	171.5	BSEE 244
300	Yes	25	41.6	2.3	199.7	175.3	2.0	2.3	151.6	BSEE 134
300	Yes	14.7	44.8	1.6	204.6	182.9	2.1	2.2	148.5	BSEE 154
300	Yes	34.8	39.5	2.7	181.5	156.0	2.4	2.5	174.2	BSEE 239
300,5	No	0.8	3.4	0.1	199.8	175.0	-	-	-	BSEE 141
300,5	No	1.6	2.8	0.1	198.5	175.9	-	-	-	BSEE 153

Ign.=ignition, P_{\max} =maximum pressure, Flr.=floor, Ext.= External location for the heat flux gauge, T_{avg} =average temperature, Horiz=horizontal, Vert=vertical, Exp=experiment ID.

* ignition delay time was not measured because the ignition was not observed in the video.

Propane – 25.0 kW Fire Size – Door Configuration – Middle Spark Position

The measurements summarized from the 25.0 kW propane fire with the door configuration and middle spark position are shown in Table 15. Fuel-off times for the 25.0 kW fire size range from 240 s to 300 s, a lower range than for the 16.7 kW propane fires with similar conditions.

Table 15. Measurements made for the 25.0 kW propane experiments with a door configuration and a middle spark position.

Fuel-off Time (s)	Ign	P _{max} (Pa)	Max Heat Flux Flr. (kW/m ²)	Max Heat Flux Ext. (kW/m ²)	T _{avg} High (°C)	T _{avg} Low (°C)	Ign. Time (s)	Horiz Flame Ext. (m)	Vert Flame Depth (%)	Exp
240	Yes	7.2	17.6	0.4	220.2	167.7	2.3	1.6	114.5	BSEE 136
240	Yes	20.9	29.2	1.0	228.5	192.3	2.0	2.0	154.3	BSEE 151
270	Yes	24.5	41.6	2.1	190.2	156.6	1.8	2.6	162.7	BSEE 138
270	Yes	18.0	50.6	1.8	209.9	184.1	2.9	2.1	165.8	BSEE 152
300	Yes	39.1	38.3	3.2	188.7	163.3	3.3	2.7	185.7	BSEE 139
300	Yes	40.7	28.4	2.7	171.7	141.6	3.8	2.6	157.0	BSEE 159
300, 5	Yes	17.4	25.5	1.8	201.8	177.4	4.8	1.7	157.0	BSEE 140
300, 5	Yes	55.0	35.7	3.4	178.8	153.0	4.6	2.5	171.5	BSEE 160

Ign.=ignition, P_{max}=maximum pressure, Flr.=floor, Ext.= External location for the heat flux gauge, T_{avg}=average temperature, Horiz=horizontal, Vert=vertical, Exp=experiment ID.

Propane – 25.0 kW Fire Size – Window Configuration – Low Spark Position

The measurements summarized from the 25.0 kW propane fire with the window configuration and low spark position are shown in Table 16. Fuel-off times for the 25.0 kW fire size range from 210 s to 300 s, a lower range than for the 16.7 kW propane fires with similar conditions.

Table 16. Measurements for the 25.0 kW propane experiments with a window configuration and a low spark position.

Fuel-off Time (s)	Ign.	P_{\max} (Pa)	Max Heat Flux Flr. (kW/m ²)	Max Heat Flux Ext. (kW/m ²)	T_{avg} High (°C)	T_{avg} Low (°C)	Ign. Time (s)	Horiz Flame Ext. (m)	Vert Flame Depth (%)	Exp
210	No	1.7	4.5	0.1	246.5	191.9	-	-	-	BSEE 196
210	No	1.8	3.5	0.1	249.6	187.8	-	-	-	BSEE 215
240	Yes	5.3	19.6	0.2	236.8	193.8	0.5	1.8	54.4	BSEE 142
240	Yes	29.7	36.3	1.4	219.6	181.3	1.4	2.3	140.1	BSEE 163
270	Yes	56.4	43.6	2.2	213.0	182.2	2.3	2.7	160.0	BSEE 143
270	Yes	40.1	35.0	0.9	210.9	181.5	2.4	2.7	171.5	BSEE 168
300	Yes	29.1	46.9	2.5	175.7	148.3	2.2	2.7	165.8	BSEE 146
300	Yes	67.6	55.3	2.7	168.3	140.5	2.5	2.9	177.3	BSEE 166
300	Yes	24.9	46.6	2.4	177.5	153.4	2.7	3.1	151.6	BSEE 195
300,5	Yes	45.7	47.8	3.6	193.4	168.9	4.7	2.7	165.8	BSEE 144
300,5	Yes	114.7	41.6	3.5	188.6	163.7	4.6	3.1	171.5	BSEE 167

Ign.=ignition, P_{\max} =maximum pressure, Flr.=floor, Ext.= External location for the heat flux gauge, T_{avg} =average temperature, Horiz=horizontal, Vert=vertical, Exp=experiment ID.

Propane – 25.0 kW Fire Size – Window Configuration – Middle Spark Position

The measurements summarized from the 25.0 kW propane fire with the window configuration and middle spark position are shown in Table 17. Fuel-off times for the 25.0 kW fire size range from 240 s to 300 s, lower than for the 16.7 kW propane fires with similar conditions.

Table 17. Measurements made for the 25.0 kW propane experiments with a window configuration and a middle spark position.

Fuel-off Time (s)	Ign.	P_{\max} (Pa)	Max Heat Flux Flr. (kW/m ²)	Max Heat Flux Ext. (kW/m ²)	T_{avg} High (°C)	T_{avg} Low (°C)	Ign. Time (s)	Horiz Flame Ext. (m)	Vert Flame Depth (%)	Exp
240	No	3.1	6.6	0.1	270.3	211.1	-	-	-	BSEE 147
240	Yes	64.0	32.6	1.0	209.1	175.8	2.7	2.7	179.9	BSEE 174
270	Yes	79.5	39.2	2.3	208.4	177.9	2.9	2.7	185.7	BSEE 148
270	Yes	142.2	42.3	3.2	168.1	138.1	0.6	3.4	160.0	BSEE 172
300	Yes	53.9	59.1	3.9	192.3	168.1	3.9	2.6	154.3	BSEE 149
300	Yes	102.2	46.0	5.2	185.8	160.9	4.4	3.1	174.2	BSEE 169
300,5	Yes	67.1	40.8	3.4	204.4	181.9	4.6	2.7	154.3	BSEE 150
300,5	Yes	71.9	60.1	4.7	188.4	163.9	4.7	2.9	179.9	BSEE 170
300,5	Yes	129.8	57.3	4.7	171.3	145.3	4.9	3.3	179.9	BSEE 173

Ign.=ignition, P_{\max} =maximum pressure, Flr.=floor, Ext.= External location for the heat flux gauge, T_{avg} =average temperature, Horiz=horizontal, Vert=vertical, Exp=experiment ID.

Propene – 25.0 kW Fire Size – Door Configuration – Low Spark Position

The measurements summarized from the 25.0 kW propene fire with the door configuration and low spark position are shown in Table 18. Fuel-off times range from 210 s to 270 s.

Table 18. Measurements for the 25.0 kW propene experiments with a door configuration and a low spark position.

Fuel-off Time (s)	Ign.	P_{\max} (Pa)	Max Heat Flux Flr. (kW/m ²)	Max Heat Flux Ext. (kW/m ²)	T_{avg} High (°C)	T_{avg} Low (°C)	Ign. Time (s)	Horiz Flame Ext. (m)	Vert Flame Depth (%)	Exp
210	No	2.2	3.3	0.1	228.4	179.0	-	-	-	BSEE 222
210	Yes	12.2	18.7	0.2	221.9	182.9	2.6	0.8	82.7	BSEE 233
210	Yes	5.2	18.2	0.2	224.0	183.0	1.3	1.0	74.3	BSEE 235
240	Yes	15.6	42.9	0.2	203.0	170.9	1.4	1.7	140.1	BSEE 223
240	Yes	7.3	57.8	0.8	199.7	169.4	1.6	2.2	165.8	BSEE 234
270	Yes	18.2	58.2	1.7	184.1	155.9	2.4	2.5	174.2	BSEE 224
270	Yes	11.5	46.2	1.6	194.8	169.1	2.1	2.1	171.5	BSEE 237

Ign.=ignition, P_{\max} =maximum pressure, Flr.=floor, Ext.= External location for the heat flux gauge, T_{avg} =average temperature, Horiz=horizontal, Vert=vertical, Exp=experiment ID.

Propene – 25.0 kW Fire Size – Window Configuration – Low Spark Position

The measurements summarized from the 25.0 kW propene fire with the window configuration and low spark position are shown in Table 19. Fuel-off times range from 210 s to 270 s.

Table 19. Measurements for the 25.0 kW propene experiments with a window configuration and a low spark position.

Fuel-off Time (s)	Ign.	P_{\max} (Pa)	Max Heat Flux Flr. (kW/m ²)	Max Heat Flux Ext. (kW/m ²)	T_{avg} High (°C)	T_{avg} Low (°C)	Ign. Time (s)	Horiz Flame Ext. (m)	Vert Flame Depth (%)	Exp
210	Yes	3.3	16.1	0.2	227.5	183.0	3.0	0.3	26.8	BSEE 229
210	Yes	10.8	29.3	0.2	205.5	160.9	1.9	1.0	54.4	BSEE 232
210	Yes	10.2	35.9	0.2	228.6	187.7	0.6	1.5	103.0	BSEE 236
240	Yes	23.4	42.6	0.4	205.6	173.1	1.7	2.8	145.9	BSEE 225
240	Yes	34.1	39.7	0.8	208.9	177.7	1.6	2.7	157.0	BSEE 230
270	Yes	17.1	56.8	0.5	190.9	163.3	2.5	2.2	119.8	BSEE 226
270	Yes	42.3	37.8	1.8	175.7	146.4	2.5	2.8	157.0	BSEE 228

Ign.=ignition, P_{\max} =maximum pressure, Flr.=floor, Ext.= External location for the heat flux gauge, T_{avg} =average temperature, Horiz=horizontal, Vert=vertical, Exp=experiment ID.

4. Conclusion

A reduced-scale compartment was constructed to study the backdraft phenomenon using three gaseous fuels: methane, propane, and propene. Backdraft events were observed under a wide range of compartment configurations. For each experiment, compartment configurations (i.e., fire size, fuel-off time, spark ignition location, spark delay time, front opening size) were changed to establish their correlation to a backdraft event. For some configurations, the compartment can repeatably create a backdraft event. Pressure, heat flux, temperature, ignition time, and flame extension measurements were made from backdraft experiments.

This report provides the experimental details of a set of backdraft experiments with methane, propane, and propene fuels. The summary data presented here provides various measurements to detail the general trends observed for the different conditions studied and for repeated experiments. Additional measurements including gaseous species in the compartment and the heat released from the backdraft events will be analyzed to provide a fuller understanding of these experiments [25].

References

- [1] Wooley WD, Ames SA (1975) "The Explosive Risk of Stored Foamed Rubber", Building Research Establishment, Current Paper 36/75, Borehamwood, UK.
- [2] Bukowski RW (1995) Modeling a backdraft: the fire at 62 Watts street", Building and Fire Research Laboratory, National Institute of Standards and Technology. NFPA J. 89 (6), 85–89.
- [3] Injuries from backdraft NIOSH Fatality Assessment and Control Evaluation Investigation Report F98-05. <https://www.cdc.gov/niosh/fire/reports/face9805.html>
- [4] NIOSH Fatality Assessment and Control Evaluation Investigation Report F98-06. <https://www.cdc.gov/niosh/fire/reports/face9806.html>
- [5] NIOSH Fatality Assessment and Control Evaluation Investigation Report F2004-17. <https://www.cdc.gov/niosh/fire/reports/face200417.html>
- [6] Fundamentals of Fire Fighter Skills, 3rd edition, NFPA, 2015.
- [7] Drysdale D, An Introduction to Fire Dynamics, Third Edition, Wiley, 2011.
- [8] Fire Engineering, "Backdraft, Mayday Declared at Troy (NY) Bowling Alley Fire", May 9, 2019. <https://www.fireengineering.com/2019/05/09/214555/troy-ny-structure-fire-2/>
- [9] Flatley C, Flashover and backdraft – a primer, Fire Engineering, March 1, 2005. <https://www.fireengineering.com/2005/03/01/272179/flashover-and-backdraft-a-primer-2/>
- [10] NFPA 921, Guide for Fire and Explosion Investigations, National Fire Protection Association.
- [11] Fleischmann CM (1994) Backdraft phenomena, National Institute of Standards and Technology, Gaithersburg, MD, NIST-GCR-94-646.
- [12] Bollinger I (1995) Full residential-scale backdraft, Master Thesis, University of Canterbury, Christchurch, NZ.
- [13] Sutherland BJ (1999) Smoke explosions, Master Thesis, University of Canterbury, Christchurch, NZ.
- [14] Weng WG, Fan WC (2003) Critical condition of backdraft in compartment fires: a reduced-scale experimental study, Journal of Loss Prevention in the Process Industries, 16: 19-26.
- [15] Weng W, Fan W (2005) Experimental study of backdraft in a compartment with different opening geometries and its mitigation with water mist, Fire Safety Science- Proceedings of the 8th International Symposium, 1181-1192.
- [16] Chen NZJ (2012) Smoke explosion in severely ventilation limited compartment fires, Master thesis, University of Canterbury, Christchurch, NZ.
- [17] Gottuk DT, Williams FW, Farley JP (1997) The development and mitigation of backdrafts: a full-scale experimental study, Fire Safety Science- Proceedings of the 5th International Symposium, 935-946.
- [18] Gottuk DT, Peatross MJ, Farley JP, Williams FW (1999) The development and mitigation of backdraft: a real-scale shipboard study, Fire Safety Journal, 33: 261-282.
- [19] Gojkovic D (2001) Initial backdraft experiments, Report 3121, Lund University, Sweden.
- [20] Tsai LC, Choi CW (2013) Full-scale experimental studies for backdraft using solid material, Process Safety and Environmental Protection, 91, 202-212.

- [21] Proposed Method for Room Fire Test of Wall and Ceiling Materials and Assemblies. American Society for Testing and Materials. Philadelphia, PA; 1982 November, 1618-1638.
- [22] Fire Tests – Full-Scale Test for Surface Products. International Standard ISO/DIS 9705. International Organization for Standardization. Geneva, Switzerland; 1991, 1-41.
- [23] Bryner NP, Johnsson EL, Pitts WM (1994) Carbon Monoxide Production in Compartment Fires — Reduced-Scale Enclosure Test Facility, National Institute of Standards and Technology, Gaithersburg, MD, NISTIR 5568.
- [24] Bundy M, Hamins A, Johnsson EL, Kim SC, Ko GH, Lenhart DB (2007) Measurements of Heat and Combustion Products in Reduced-Scale Ventilation-Limited Compartment Fires, National Institute of Standards and Technology, Gaithersburg, MD, NIST Technical Note 1483.
- [25] Falkenstein-Smith R, Cleary TG (2021) Gas species and thermal measurements preceding backdraft events in a 2/5th scale compartment, National Institute of Standards and Technology, Gaithersburg, MD, NIST Technical Note 2185.
<https://doi.org/10.6028/NIST.TN.2185>
- [26] Lautkaski R (1997) Understanding Vented Gas Explosions, Technical Research Centre of Finland (VTT), Tiedotteita - Meddelanden - Research Notes 1812.
- [27] NOAA website, “Overpressure Levels of Concern”, last updated April 17, 2019
<https://response.restoration.noaa.gov/oil-and-chemical-spills/chemical-spills/resources/overpressure-levels-concern.html>
- [28] Harris RJ, Wickens MJ, Johnson DM (1985) The effect of explosion pressures on structures and structural components. In: A Practical Introduction to Gas and Dust Explosions, A Two Day European Seminar, Frankfurt, 3-4 June 1985. Hove: European Information Centre for Explosion Protection. Part 1. 15 p. + app. 7.
- [29] Samali B, Mckenzie G, Zhang C, Ancich E (2018). Review of the Basics of State of the Art of Blast Loading. Asian Journal of Civil Engineering. 1-17.
- [30] 80/20, Inc., website, deflection calculator, <https://8020.net/deflection-calculator>
- [31] The Engineering Toolbox (www.engineeringtoolbox.com)
- [32] Incropera FP, Dewitt DP, Bergman TL, Lavine AS (2007) Fundamentals of Heat and Mass Transfer, 6th edition, John Wiley and Sons, Inc., Hoboken, NJ
- [33] SFPE Handbook of Fire Protection Engineering, National Fire Protection Association, Zalosh, R, p 2745.
- [34] NFPA 68, Standard on Explosion Protection by Deflagration Venting, National Fire Protection Association.

Appendix A: Design Document Details

The Performance Design Basis for a Reduced-Scale Backdraft Compartment

Purpose

The purpose of this document is to provide the detailed calculations that were used to design the reduced-scale compartment (RSC). The three main design aspects of the compartment that are reported here include:

- the design of the pressure relief panel,
- the design of the aluminum support structure,
- the design of the composite compartment wall

These calculations were documented to report the assumptions made with the design of the RSC and to understand the limitations and usable criteria for the compartment for safe and repeatable use for backdraft experimentation. This report will also allow future users to decide if the RSC is safe to use as experimentation is modified.

Requirements

The compartment was designed with safety factors to allow the RSC to be safely reused. Assumptions were made with high estimates of heat and pressure based on previous literature. These estimates were used to design the RSC for repetitive use under the normal expected conditions. The compartment was also designed to safely sustain an unusual event where temperature and pressure reached extreme levels.

Compartment Dimensions

The reduced-scale compartment was a rectangular enclosure. The dimensions were 1 m (height) x 1 m (width) x 1.5 m (length) and were a similar size as the reduced-scale enclosure documented in Bryner et al. (1994) [23] and Bundy et al. (2007) [24]. These dimensions were chosen to be a two-fifths scale of the ISO/ASTM standard full-scale test room (2.44 m x 2.44 m x 3.66 m) [21, 22].

Deflagration versus Detonation

Deflagration is the propagation of combustion of fuel and pressure below the speed of sound, whereas detonation is the propagation of combustion and pressure faster than the speed of sound [26].

Compartment Influences

Various features of the compartment that contain the deflagration may affect the speed and pressure of the pressure wave and flame front [26]. The compartment size and shape affect the pressure. The overpressure developed within a compartment is inversely proportional to the size of the compartment, and also increases within a cubic-shaped compartment. The

smoothness of the interior compartment walls, the emptiness of the room, and the centered location of a vent each affect the overpressure in the compartment. Obstacles within the compartment create turbulence in the unburned gas mixture, which accelerates and enlarges the flame front [26]. Turbulence within the RSC will be minimized with only a few obstacles. When gas fuel is used, the gas fuel burner and ignitor will be within the compartment. If solid fuel is used, a platform will hold the solid fuel supported by four legs that pass below the platform. Several sensors will extend into the interior of the compartment, and also along the walls of the compartment but are not expected to create much turbulence.

A stoichiometric mixture of gas fuel and air results in the potential for the greatest explosion from overpressure, a worst-case scenario [26].

Summary of pressure damage

Several references correlate structural damage with blast pressures, as seen in Table 20. In general, pressures of 0.69 kPa (0.1 psi) cause residential windows to crack. Pressures up to 6.9 kPa (1 psi) can cause glass windows to shatter, minor interior residential home structural damage, and interior room door failure. Pressures up to 34.5 kPa (5 psi) can cause major exterior residential home structural damage.

Table 20. Expected structural damage based on overpressures.

Overpressure kPa (psig)	Expected Damage (NOAA, 2019) [27]	Expected Damage (Harris et al, 1985) [28]	Expected Damage (Samali et al, 2018) [29]
< 1 (0.15)	Typical pressure for glass failure		Typical glass window damage
< 3 (0.4)	Limited minor structural damage	Failure of room doors	
< 5 (0.7)	Minor damage to house structure	Failure of light partition walls, 50 mm thick breeze block walls	
< 7 (1)	Partial demolition of houses	Glass window failure	Minor damage to buildings
< 14 (2)	Partial collapse of walls and roofs of houses.	Unrestrained brick walls	
< 17 (2.5)	50 % destruction of home brickwork		
< 21 (3)	Steel frame buildings distorted and pulled away from foundation		Failure of concrete blockwork
< 34 (5)	Wood utility poles snapped		Serious damage to steel framed buildings

A1. Design of Structure Integrity (maximum overpressure requirement)

Detailed Compartment Drawings

The RSC was designed to be reused for experimental work involving elevated temperatures and pressure within the compartment. The frame of the compartment must be able to withstand the temperatures and pressures that are expected within the compartment. Temperatures on the exterior of the compartment where the aluminum studs were located were not expected to exceed 150 °C.

The reduced-scale compartment was a 99 cm high, 99 cm wide, 152 cm long rectangular box. The interior layer of the compartment was a 2.54 cm thick ceramic board surrounded by a 3 mm ceramic fiber paper for thermal protection. The ceramic board was attached to a 1 cm thick sheet of aluminum. The aluminum sheet was attached to a frame of aluminum bars.

Bar Material Property

The 6105 aluminum alloy bars that make the framework of the compartment were used on all sides. Although the modulus of elasticity, E , for a material typically changes with temperature, the temperature range expected for the aluminum parts of the compartment (up to 200 °C) will not be high enough to cause a change in elasticity to impact these calculations. Therefore, the elasticity of the aluminum alloy at room temperature, 70 GPa [30], was used.

Bar Geometry

The vertical and horizontal bars were fixed at both ends, attached to the corner beams, using gusset plates. The bars were 1 m in length, L , with a rectangular cross section of 2.54 cm by 5.08 cm. The bar cross section was positioned so that the shorter side, 2.54 cm, was receiving the load. The perpendicular distance from the surface of the bar to the neutral axis on the bar cross section (y), was 25.4 mm. The moment of inertia, I , based on the geometry and position of the cross section, was 12.8 cm⁴ [31].

Force on bar

The force applied to the aluminum bars will be due to an internal pressure in the compartment. The internal pressure applied to the compartment may be up to 6.9 kPa (1 psi) during a deflagration event, but the elevated pressure is not expected to be a sustained pressure but rather a pressure burst. The pressure relief panel will open at a pressure of 0.69 kPa (0.1 psi), however the pressure wave may elevate the internal pressure to 6.9 kPa (1 psi) while the relief panel is opening. Once the pressure relief panel is opened the experiment is over.

For safety purposes, the compartment was designed to withstand an extreme internal pressure of 34.5 kPa (5 psi) although pressures this high were not expected. Therefore, calculations were done to determine the bar deflections and bending stress in the frame bars during an extreme temperature and pressure event within the compartment.

The internal pressure is applied to the inside wall of the compartment, a section of the wall on either side of a bar will be transferred to the bar itself. The section of wall receiving the load was therefore 244.5 mm wide by 1000 mm long or 244,500 mm².

The internal pressure was assumed to be applied uniformly and continuously to the internal surface of the compartment.

For a 6.9 kPa (1 psi) internal pressure transferred to a surface 244500 mm², the load applied, F, to the 25.4 mm wide 1000 mm long bar will be 1686 N. For a 34.5 kPa (5 psi) internal pressure, the load, F, will be 8428 N.

Assumptions for 6105 aluminum alloy bar:

- Beam is loaded continuously and uniformly
- Beam has fixed ends
- E = 70 GPa
- I = 12.8 cm⁴
- L = 1000 mm
- F = 1686 N for 6.9 kPa (1 psi), and 8428 N for 34.5 kPa (5 psi)
- y = 25.4 mm

Beam deflection

The equation to calculate the maximum deflection of a beam with fixed ends under a uniform load is [31]:

$$d = F L^3 / (384 E I) \tag{1}$$

The maximum deflection at the mid-point of the beam will be 0.49 mm for a 6.9 kPa (1 psi) internal pressure or a deflection of 2.44 mm at an internal pressure of 34.5 kPa (5 psi).

Bending Stress

To calculate the maximum bending stress, which occurs at the midpoint of the bar with fixed ends, the following equation is used [31]:

$$\sigma = F L y / (24 I) \tag{2}$$

The maximum bending stress at the mid-point of the beam will be 13.9 MPa at a 6.9 kPa (1 psi) internal pressure, or a maximum bending stress of 69.6 MPa at an internal pressure of 34.5 kPa (5 psi). The yield strength for this material at room temperature is 241 MPa. Since the maximum bending stress is well below the yield strength, the aluminum will remain in the elastic range even at the elevated pressure of 34.5 kPa (5 psi).

Summary

Theoretical maximum deflection and maximum bending stress of the aluminum bars are shown in Table 21.

Table 21. Theoretical maximum deflection and maximum bending stress of the aluminum bars based on an internal pressure of 6.9 kPa (1 psi) and an extreme internal pressure of 34.5 kPa (5 psi).

Internal Pressure kPa (psi)	Maximum Deflection (mm)	Maximum Bending Stress (MPa)
6.9 (1)	0.49	13.9
34.5 (5)	2.44	69.6

A2. Design of Thermal Protection

The RSC needs sufficient thermal protection to maintain the structural integrity of the aluminum frame and walls to allow the RSC to be safely reused for multiple experiments. Therefore, the design goal was to limit the aluminum structural elements to temperatures below 100 °C. The following description using steady-state heat and other assumptions calculates the theoretical temperatures outside the RSC aluminum wall.

The RSC is a rectangular box, 1 m high, 1 m wide, and 1.5 m long. The inner surface of the enclosure will be covered with a low-density ceramic board to provide thermal protection for the enclosure (Fig. 39). The ceramic board is attached to an aluminum sheet and aluminum bar frame to provide the board with structural strength.

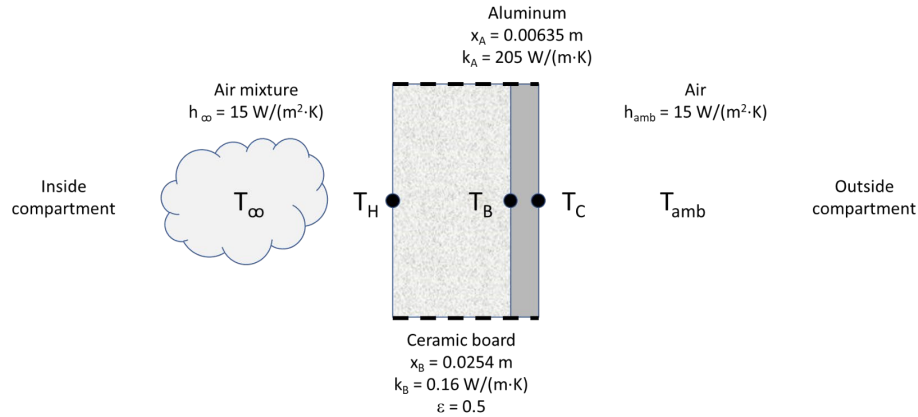


Fig. 39. The one-dimensional plane composite wall for the compartment with the ceramic board as the interior layer of the enclosure and aluminum as the structural support. The heat source is on the inside of the enclosure.

Assumptions:

Steady-state conditions

One dimensional heat transfer

Ceramic Board

The emissivity of the ceramic board, $\epsilon = 0.5$

Uniform thermal conductivity for ceramic board, $k_B = 0.16 \text{ W}/(\text{m}\cdot\text{K})$

Ceramic board thickness, $x_B = 0.0254 \text{ m}$

Aluminum wall

Uniform thermal conductivity for aluminum, $k_A = 205 \text{ W}/(\text{m}\cdot\text{K})$

Aluminum thickness, $x_A = 0.0095 \text{ m}$

Temperatures

Hot atmosphere within the enclosure, $T_\infty = 1000 \text{ }^\circ\text{C}$

Ambient temperature on the cold side of the wall, $T_{\text{amb}} = 20 \text{ }^\circ\text{C}$

Convection heat transfer coefficient for air, for the air mixture within the enclosure h_∞ and air outside the enclosure h_{amb} , $= 15 \text{ W}/(\text{m}^2\cdot\text{K})$.

Stefan-Boltzmann constant, $\sigma = 5.67 \times 10^{-8} \text{ W}/(\text{m}^2\cdot\text{K}^4)$

Contact resistance between the two materials is negligible.

Heat rate q is the same through both materials.

Heat Transfer to the Inside Wall

The following equations were used [32]. For the heat transfer from inside the enclosure, including convection and radiation, the heat rate per unit area, q/A , was calculated using:

$$q/A = q/A \text{ radiation} + q/A \text{ convection} \tag{3}$$

where: $q/A \text{ radiation} = \epsilon\sigma (T_\infty^4 - T_H^4)$

$$q/A \text{ convection} = h_{\infty} (T_{\infty} - T_H)$$

Conduction through Ceramic Insulating Wall

For conduction through the 2.54 cm ceramic board, the q/A is assumed to be the same, and the following equation was used:

$$q/A = k_B (T_H - T_B) / x_B \tag{4}$$

Conduction through Aluminum Wall

For the heat conduction through the 0.95 cm aluminum, the following equation was used:

$$q/A = k_A (T_B - T_C) / x_A \tag{5}$$

Heat Transfer from the External Wall

Lastly, for the convection and radiation from the outside surface of the aluminum to the 20 °C ambient air:

$$q/A = h_{amb} (T_C - T_{amb}) + \epsilon \sigma (T_C^4 - T_{amb}^4) \tag{6}$$

Results

Based on previous literature, the interior enclosure temperature, T_{∞} , could be as high as 1000 °C. Table 22 shows a range of interior RSC temperatures and the resulting theoretical exterior temperatures of the aluminum wall (T_C) as determined by the equations. Additional cooling of the exterior of the RSC with fans or increasing the thickness of the ceramic board could further lower the exterior aluminum wall temperature.

Table 22. A range of steady-state interior compartment temperatures and the resulting theoretical exterior wall temperatures.

Interior Compartment Temp, T_{∞} (°C)	Theoretical Exterior Aluminum Wall Temp, T_C (°C)
1000	158
900	144
800	131
700	118
600	103

A3. Design of Pressure Relief Panel

The primary hazards beyond routine compartment fire experiments were the compartment overpressures experienced during backdraft or smoke explosions. The compartment structure and pressure relief system design goal was to mitigate excessive overpressures during events that could pose a safety hazard or damage the compartment. The methodology to meet this goal was to specify and justify the performance criteria, then detail the design features that met these criteria.

During an experiment, a pressure relief panel was used to mitigate excessive overpressures during events that could pose a safety hazard or damage the compartment. The design goal was to relieve the potential overpressure from a deflagration of a stoichiometric mixture of propane and air inside the reduced-scale compartment. At ambient temperature, such a mixture can produce an overpressure of 700 kPa, (100 psig) which would be very difficult to contain in a rectangular compartment. It should be noted here that this overpressure is much higher than any potential unrelieved overpressure expected during these experiments as described. Also, a detonation or deflagration to detonation transition (DDT) is not considered a possibility due to the configuration (scale), fuels considered, and ignition source strength.

Limiting structural damage (no permanent deformation of the structure) imposes a much stricter overpressure limit than structural failure, i.e., the safety hazard limit. Thus, the blowout panel design goal here is to keep the compartment overpressure below 6.9 kPa (1 psi). This is the overpressure limit where windows are usually shattered, whereas an overpressure of 34.5 kPa (5 psi) is sufficient to eradicate a home [33]. This constrains the structure to a design that can withstand this force without deforming at the expected elevated temperatures during the experiments.

When combustion begins and the fuel-air mixture ignites deflagration, the pressure rises within the enclosure. When the pressure meets the designed opening pressure of the enclosure vent, P_v , the vent opens, venting unburned gas, and the pressure peaks for the first time and then decreases. As the flame front continues, unburned gas vents from the enclosure, the flame front reaches the vent opening and ignites and vents with a pressure peak, P_{red} . This pressure vents from the enclosure resulting in a second pressure decrease [26].

The following describes the pressure relief panel design for the RSC following the Low Strength Method for Enclosures from NFPA 68-2018 (Standard on Explosion Protection by Deflagration Venting) [34]. “This standard applies to the design, location, installation, maintenance, and use of devices and systems that vent the combustion gases and pressures resulting from a deflagration within an enclosure so that structural and mechanical damage is minimized.” The goal of the standard is to determine the vent size for enclosures where deflagrations may occur. Based on the enclosure size, fuel, and vent, the minimum vent size is calculated.

The first step for using NFPA 68 to determine the vent size opening is to consider initial conditions. The RSC was a rectangular enclosure with one vent at one end with no hopper extension. The overall compartment dimensions were 1 m high, 1 m wide, and 1.5 m long. The fuel for these calculations was propane with a fundamental burning velocity of the gas-air mixture (S_u) as 0.46 m/s.

The initial pressure within the enclosure before ignition (P_0) was assumed to be 0 kPa. The peak pressure for the RSC, P_{red} , defined as the maximum pressure developed in a vented enclosure during a vented deflagration, was 6.9 kPa (1 psi). For use in the calculations, the maximum pressure developed in a contained deflagration by ignition (P_{max}) was 790 kPa (115 psi), and the stoichiometric volume fraction for propane fuel in air (X_{st}) was 0.055.

The calculations to determine the vent area were based on Chapter 7 of NFPA 68 [34], venting deflagrations of gas mixtures and mists. Since the theoretical mass per area of the vent panel, M , 30 kg/m², was less than the 40 kg/m² threshold, the minimum required vent area calculation (A_{v2}) was used for low pressure, and a low-inertia vent was used with the assumptions that there was one vent ($n=1$), it was hinged ($F_{SH}=1.1$), and the vent will be the entire wall ($C_d=0.8$):

$$A_{v2} = A_{v1} \times F_{SH} \left[1 + \frac{(0.05) \times M^{0.6} \times (S_u \times \lambda)^{0.5}}{n^{0.3} \times V \times P_{red}^{0.2}} \right] \quad (7)$$

where A_{v1} is the partial volume deflagration, λ is the turbulent flame enhancement factor related to the surface area of obstructions within the compartment, S_u is the fundamental burning velocity of the fuel, and V is the enclosure volume.

Based on these calculations for the enclosure's size, vent mass, and fuel, the minimum vent area, A_{v2} , was 0.9 m² so that the maximum pressure within the RSC, P_{red} , did not exceed 6.9 kPa (1 psi). Since the back wall of the enclosure was 1 m², the entire wall was hinged and served as the pressure relief panel. The panel was set to open at a pressure of 0.69 kPa (0.1 psi) (P_v), well below the maximum pressure designed for the compartment during a vented deflagration (P_{red}) of 6.9 kPa (1 psi).